Design and Analysis of Three Phase PFC Converters for More Electric Aircraft Applications

A Project Report

submitted by

N VISHNU SAI

EE18M090

in partial fulfilment of requirements

for the award of the degree of

MASTER OF TECHNOLOGY

DEPARTMENT OF ELECTRICAL ENGINEERING

INDIAN INSTITUTE OF TECHNOLOGY MADRAS

MAY 2020

THESIS CERTIFICATE

This is to certify that the thesis titled **Design and Analysis of Three Phase PFC Converters for More Electric Aircraft Applications** , submitted by **N VISHNU SAI (EE18M090)**, to the Indian Institute of Technology, Madras, for the award of the degree of **Master of Technology**, is a bonafide record of the research work done by him under my supervision. The contents of this thesis, in full or in parts, have not been submitted to any other Institute or University for the award of any degree or diploma.

Dr. Lakshminarasamma N
(Project Guide)
Associate Professor
Department of Electrical Engineering
IIT-Madras, 600 036

Place: Chennai

Date: 14/06/2020

ACKNOWLEDGEMENTS

First and foremost I want to thank my guide Prof. Lakshminarasamma madam for accepting me as her student and giving opportunity to do work in Power Electronics Simulation Laboratory . She was very supportive and gave complete freedom right from the beginning. She made sure that I didn't fall short of anything through out the project. I am grateful to madam for her continual support and invaluable advice during the project.I am really fortunate to be her student. I would like to thank everyone in the Power Electronics Simulation Laboratory for imparting their knowledge with me.

I would also like to thank Harish Sudhakaran Nair my lab mate, a PhD scholar working under Lakshmi madam. He gave many insights and alerted me about many aspects in hardware implementation. His experience and knowledge in the field of PFC converters was helpful in various stages of this project and played a crucial role in moving this project forward.

I want to thank Prakash, for providing me the basic knowledge in the PCB design. Another person I would like to thank is Bishal Mondal a PhD scholar, He was my go to person if I need any kind help. He clarified many technical doubts of mine. It would be disregardful if I don't mention Vivek, Kuldip and Nitheesh my labmates who had shown some interest in my project which really motivated me to continue this work with enthusiasm. There are simply no words to express how grateful I am for the wonderful set of friends and classmates I have at IIT Madras. I would like to thank each and everyone in my life for their never-ending support and encouragement they gave me when I needed it the most.

ABSTRACT

KEYWORDS : More Electric Aircraft ; Continuous Conduction Mode(CCM) ; Discontinuous Conduction Mode(DCM)

To improve efficiency and to reduce the environmental impact of aircraft, global efforts for reducing the aircraft weight are underway. One of the key issue is the use of electric systems instead of heavy mechanical, pneumatic, and hydraulic driven systems. This change in the power supply structure of an aircraft is known as More Electric Aircraft (MEA). In the course of this concept, unidirectional active three-phase rectifiers in the power range of several kW are required, mainly for electrically driven actuators for flight control.

In modern civil aircraft a three-phase AC mains with a voltage level of either 110 V or 200 V with $\pm 15\%$ variation and a variable mains frequency of 350 - 800 Hz exists. This existed variable frequency necessitates power electronic converters to convert variable frequency AC to constant DC with high power quality and reliability with less number of components and sensors.

A numerous three-phase PFC converter topologies are reported in the literature to improve power quality. The popular topologies for AC-DC conversion are a buck, boost, and buck-boost type rectifiers that have a high level of power quality at both input and output ends. In MEA, since the DC-link voltage magnitude is greater than the peak input AC voltage magnitude, either boost or buck-boost type of rectifiers are the suitable choice for AC-DC rectification.

The three-phase two-level six switch boost type rectifier and the six switch Vienna-type rectifier are the conventional topologies and has been widely discussed in the literature. These converters are operated in continuous conduction mode and require two control loops; one is to regulate the output voltage and the other is to shape the input current sinusoidal. Hence, the control algorithm requires at least five sensors (two

input voltages, two input currents, one output voltage) for its implementation. These converters also require more switching components which increases the losses.

In the thesis, a case study of a three-phase buck-boost PFC converter with inductors connected in star and delta topologies are analysed. Detailed analysis of the modes of operation, modeling, control, comparison, and design aspects are discussed. These topologies are operated in Discontinuous Conduction Mode which makes the control algorithm simple and also avoids the need of current control loop, thus reducing the number of sensors in the hardware implementation. Both the converter topologies are simulated in MATLAB/SIMULINK and relevant waveforms of the converters are presented.

TABLE OF CONTENTS

LIST OF TABLES

LIST OF FIGURES

ABBREVIATIONS

APU	Auxiliary Power Unit
ATRU	Auto Transformer Rectifier Unit
ATU	Auto Transformer Unit
CCM	continuous Conduction Mode
DCM	Discontinuous Conduction Mode
IDG	Integrated Drive Generator
MEA	More Electric Aircraft
PFC	Power Factor Correction
PEC	Power Electronic Converter
THD	Total Harmonic Distortion
TRU	Transformer Rectifier Unit

NOTATION

v_a, v_b, v_c	Input phase voltages
v_{ab}, v_{bc}, v_{ca}	Input line voltages
i_a, i_b, i_c	Input phase currents
L_a, L_b, L_c	Input inductances
i_{La}, i_{Lb}, i_{Lc}	Input inductor cuurents
$i_{Lap}, i_{Lbp}, i_{Lcp}$	Peak value of inductor cuurents at the end of mode-1
$i_{Las}, i_{Lbs}, i_{Lcs}$	Peak value of inductor cuurents at the end of mode-2
V_o	Output voltage
i_{do}	Output current before output capacitor
i_o	Load current
i_c	Output filter capacitor current
t_{on}	On time period of the switch
t_s	Time duration of mode-2
t_r	Time duration of mode-3
t_d	Time duration of mode-4
T_s	Time period of one switching cycle
$D = \frac{t_{on}}{T_s}$	Duty cycle of the switch
V_m	Peak value of input phase voltage
I_m	Peak value of input phase current
$V_{m,min}$	Minimum value of phase input peak voltage
$V_{m,max}$	Maximum value of phase input peak voltage

f	Line frequency
f_s	Switching frequency
$M = \frac{V_o}{V_m}$	Voltage conversion ratio
M_{cr}	Critical voltage convertion ratio
$i_{o,avg}$	Switching cycle average output current
$I_{o,avg}$	Line period average output current
G_{vd}	Uncompensated voltage loop gain transfer function
G_{pi}	Compensator transfer function
$G_{vd}G_{pi}$	Compensated voltage loop transfer function
K_p	Proportional constant
K_i	Integral constant
$\overline{v_a}(t)$	Average value of input phase voltage
$\overline{i_a}(t)$	Average value of input phase current
$E_{mag}(t)$	Energy stored during magnetisation interval in the inductors
V_{MN}	Common mode voltage

CHAPTER 1

Introduction

1.1 Motivation

The More Electric Aircraft (MEA) – a step in the direction of a more energy-efficient aircraft. The concept of More Electric Aircraft (MEA) implies increasing the use of electrical power to drive aircraft subsystems. However, in the conventional aircraft system, subsystems are driven by a combination of mechanical, hydraulic, and pneumatic systems. These non-electrical systems are very bulky and less efficient. Therefore, the main objective of the MEA is to replace these non-electric systems in the aircraft with electrical systems. The key benefits of replacing non-electrical systems with electrical systems include improvement in fuel efficiency, reduction in environmental impacts and the major advantage being the reduction in the total weight of the aircraft.

However, the major concern is that more electrical systems in MEA requires more electrical power to be generated in the aircraft. With increase in the consumption of electrical power in aircraft motivates us to use more efficient electrical power conversion technologies. Therefore, power electronic converters play an important role in enabling aircraft industries to move towards MEA.

1.2 Aircraft Power Systems

The main functions of electrical power systems in the aircraft are generation, regulation, transmission, distribution, storage, and utilization. Performance of the aircraft directly related to the reliability of the electrical power systems. Generally, aircraft systems and subsystems use both AC and DC power. The main sources of electrical power in the aircraft are generators, these are mainly driven by the engine. Apart from generators, aircraft also consists of multiple supplemental sources as redundancy.

In conventional aircraft, the engine is connected to an electrical generator through a mechanical drive called Integrated Drive Generator(IDG), this drive keeps the mechanical speed of the generator constant from a variable speed input. The electrical generator generates an AC output of fixed voltage and fixed frequency [1].

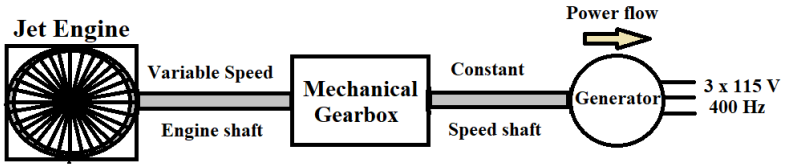

Figure 1.1: Conventional electrical power generation

In MEA engine is directly connected to a generator without any mechanical drive, so the generator output will be an AC voltage with variable frequency. Removal of mechanical drive in MEA results in a significant reduction in the weight of the aircraft.

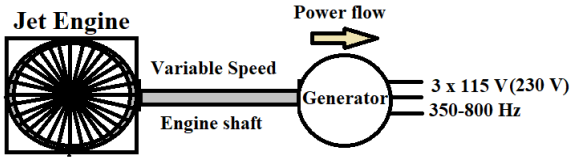

Figure 1.2: MEA electrical power generation by removing mechanical drive

Fig 1.3 shows the electrical power systems in typical More electric aircraft [2]. One of the enabling technologies for MEA is power electronic converters. Various types of power electronic converters such as AC-DC, AC-AC, DC-DC are required for different loads operating at different voltage levels in an aircraft system. In the thesis mainly AC-DC converters are discussed.

The two important design objectives of the power electronic converters for aircraft systems are power density and reliability. Moreover, the input power quality for the AC-DC converter should also meet the required aircraft standards. Further, the PEC's are required to be operated in harsh environmental conditions. Therefore, it is important that the reliability aspects of the converter are not compromised in the process of achieving high power density.

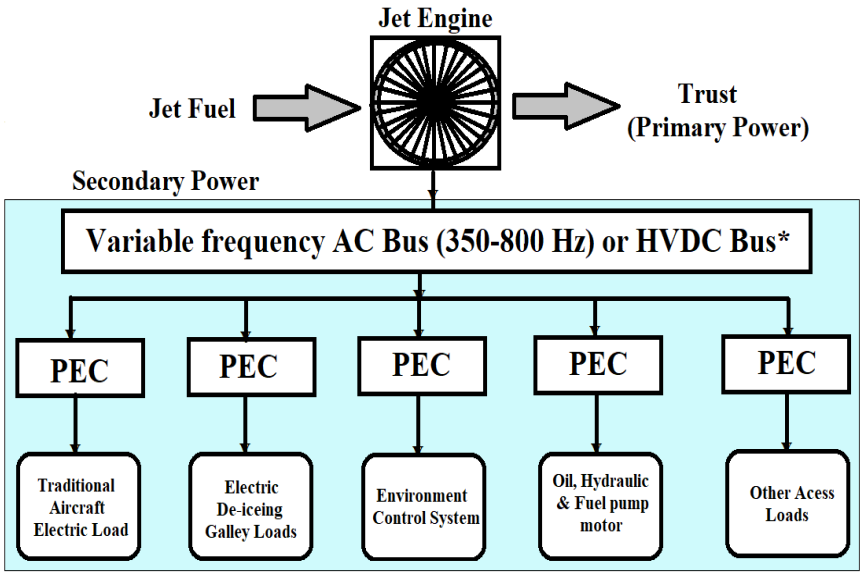

Figure 1.3: A typical More Electric Aircraft

1.3 Power Electronic Converters in MEA

Various types of power electronic converters are used in aircraft system for converting electrical power from one voltage level to other voltage level.

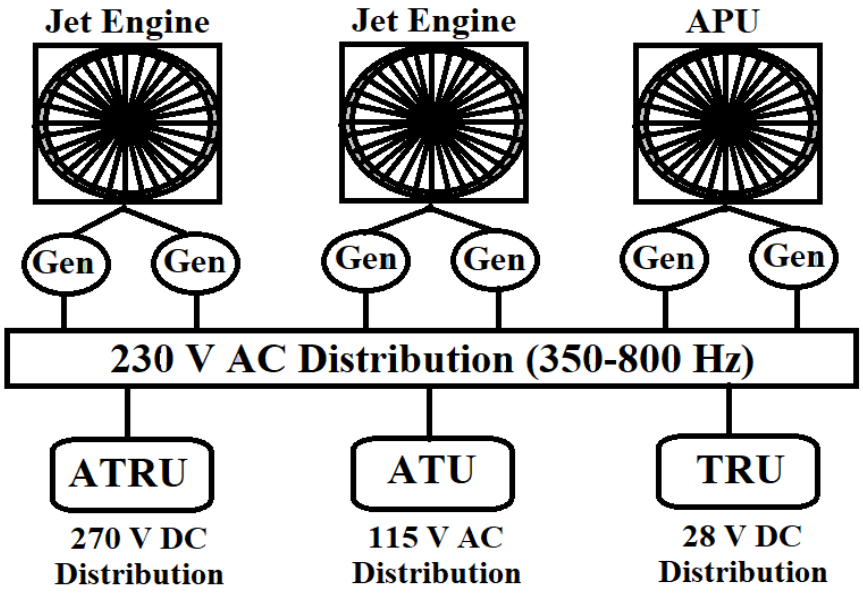

Figure 1.4: Electrical power distribution in MEA Boeing 787

Fig 1.4 shows the Electrical power distribution in Boeing 787 which is More Electric aircraft [2]. It consists of two jet engines and one Auxiliary power Supply Unit (APU). Each jet engine drives two generators of rating 250 kVA. APU is used to supply power when aircraft are in-ground and main engines are in shutdown. APU also drives two generators of rating 225 kVA. Each generator generates an output of 230 V AC of variable frequency 360-800 HZ. The output voltages of the generators are regulated by Automatic Voltage regulators (AVR). The introduction of variable frequency generation presents new challenges for power electronic converters to maintain high power quality and reliability. The aircraft system consists of different types of loads, each load requires different input voltage levels of both AC and DC.

From Fig 1.4 Auto Transformer Rectifier Unit (ATRU) is a non-isolated three-phase AC-DC passive rectifier that converts fixed voltage variable frequency AC generated by the aircraft generators into DC voltage. The Auto Transformer Unit (ATU) is essentially an AC-AC converter that steps down the high voltage AC to low voltage AC. The Transformer Rectifier Unit (TRU) rectifies fixed voltage variable frequency AC voltage into low voltage DC with electrical isolation.

The thesis mainly deals with AC-DC power conversion rectifiers for the Aircraft system. So the focus is mainly on ATRU and TRU of the aircraft system. AC-DC power conversion can be done in two ways

1) Passive power conversion

2) Active power conversion

1.4 Comparison of Passive and Active Power Conversions in Aircraft

Passive power conversion shows some benefits when compared to active power conversion in terms of simplicity and control complexity. ATRU and TRU are passive power converters which consist of a three-phase diode bridge. ATRU and TRU have more weight due to Auto-transformer/ transformer units. Moreover, the output voltage in passive systems mainly depends on mains and load variations which is one of the main drawbacks besides weight.

The above mentioned drawbacks can be overcome by using active power conversion systems such as PWM AC-DC rectifiers. By operating the active switches at a high-frequency significant reduction in the weight of the system can be achieved. The control of the switches in the active rectifier allows regulated output voltage with superior input power quality. However, the relative complexity of practical realization and control are still issues in active rectifiers.

The current passive rectifiers like ATRU and TRU can be replaced with active rectifiers of non-isolated and isolated AC-DC converters respectively. In an aircraft system, unidirectional AC-DC converters are required as there is no need of power to flow from load to source.

1.5 Limitations of Buck and Boost Rectifiers

For the given input voltages of 110 V and 200 V AC, the Buck, Boost and Buck-Boost converters provide more efficient AC to DC conversion with superior input power quality. But buck and boost converters have a limit over the maximum and minimum output voltage respectively. Fig 1.5 shows the characteristics of Boost and Buck three-phase rectifiers plotted by Considering the source RMS voltage,$V_{in,rms}$ to vary from 0-250 V, the output voltage of the converters are plotted for modulation index(m) =1. Therefore from Fig 1.5, it is clear that some voltage range which does not fall between the range of buck and boost converters, for these types of applications requires three-phase buck-boost rectifiers [2].

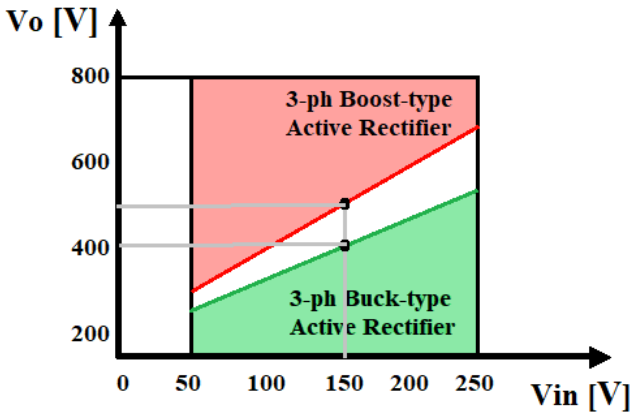

Figure 1.5: Buck and Boost characteristics of three phase rectifiers

In the active AC-DC rectifier, three-phase Buck-Boost rectifiers are used widely alternative to a diode bridge rectifier, as they provide several benefits including Power Factor Correction(PFC), reduced THD in the input current and constant regulated DC output voltage even under input voltage and output load fluctuations.

1.6 Organisation of Thesis

Chapter 2 presents the comparison of some of the popular three-phase PFC topologies, and limitations of these topologies for the aircraft applications are discussed.

Chapter 3 presents the three-phase buck-boost derived PFC converter with inductors connected in Δ-configuration, operated in DCM. Detailed analysis of design, modes of operation, modeling,small-signal analysis of the converter is discussed in this chapter.

Chapter 4 presents the design of the PI controller, and design parameters are calculated for the mentioned specifications in this chapter.

Chapter 5 presents the simulation results of 2 kW, 400 Hz, 110 V AC RMS/ 270 V DC Three phase buck-boost PFC converter.

Chapter 6 presents the state-of-the-art topology with inductors connected in Y-configuration and also presented the extension to the state-of-the-art topology to mitigate the problems of Common mode voltage and high voltage stress in switches present in the base topology. A detailed analysis of the converter is presented in this chapter.

Chapter 7 presents the simulation results of 2 kW, 400 Hz, 200 V AC RMS/ 270 V DC converter with Y-configuration. problems with the base topology are solved in the extension topology and the same is validated in the simulation.

Chapter 8 presents the comparison of two topologies with Δ and Y-connected inductors. It also gives an outlook on further research that can be carried out based on this thesis.

CHAPTER 2

Comparison of Converter Topologies in the Literature

The main goals of More electric aircraft are weight reduction, engine emission reduction, reduced fuel consumption, noise reduction which makes air travel more efficient and environmental friendly. To achieve these goals most of the non-electrical systems should be replaced with electrical systems since, electrical energy is cleaner, quieter, flexible, reliable, and most efficient.

Also, in MEA the heavy mechanical gearbox called integrated drive generator (IDG) is absent and the generator is directly connected to the main engine, thereby resulting in variable frequency mains of 350 to 800 Hz. Here, the power electronic converters play a vital role in the conversion of variable frequency AC to constant output DC with high power quality and reliability with less number of components and sensors.

2.1 Role of Active PFC Converters

It is reported that the active PFC converters enable the potential for future more electric aircraft due to their higher power density, better input power quality, and constant regulated DC voltage. Numerous three-phase PFC rectifier topologies were reported in the literature to improve power quality. The popular topologies for AC to DC conversion are Buck, Boost, Buck-Boost type Active PFC converters which have a high level of power quality at both input and output sides.

In MEA the output voltage at the DC bus is greater than the peak input AC voltage therefore either Boost or Buck-Boost type rectifiers are suitable for AC-DC conversion.

2.2 Popular PFC Converter Topologies in the Literature

2.2.1 Six Switch Boost PFC Converter

Today, active three-phase PFC rectifiers need to meet very challenging performance requirements. In most of the applications, the input current of active three-phase PFC rectifiers is required to have a total harmonic distortion (THD) less than 5% and the Power factor should be greater than 0.99. One of the most cost-effective topologies that can meet these requirements is the three-phase six-switch boost PFC rectifier.

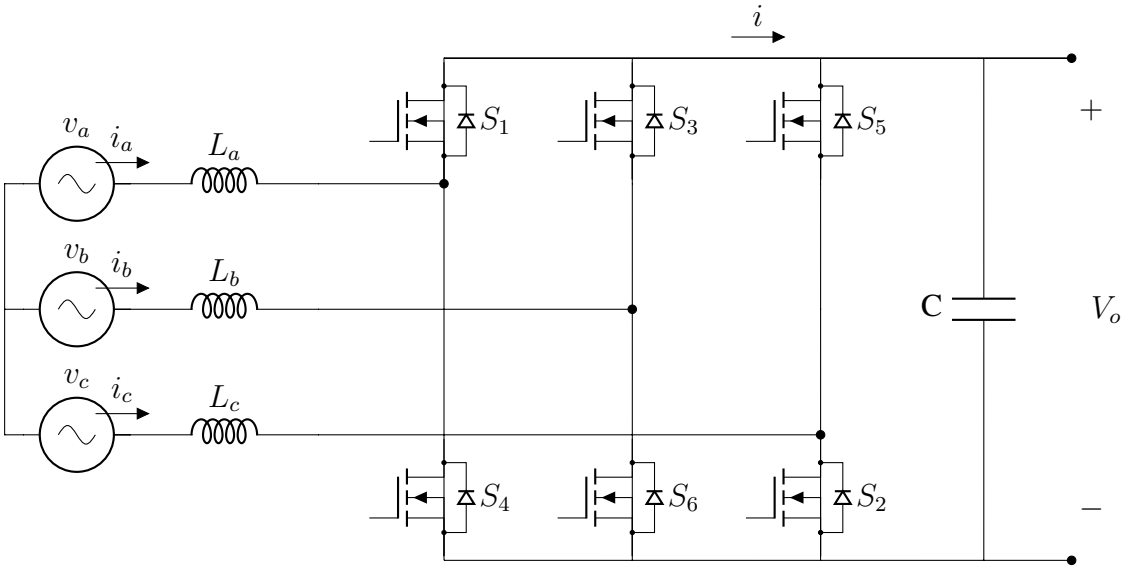

Figure 2.1: Six switch Boost PFC converter circuit topology

In three-phase applications, the six-switch boost PFC rectifier [3] is the most widely employed topology because of its simple structure, high functionality, and cost-effectiveness. But it has some limitations in aircraft applications.

Limitations:

- It has limitations over minimum output voltage.
- For aircraft application switching frequency will be high, which increases the switching losses as six switches are used.
- Bidirectional rectifiers are not suitable for aircraft applications
- Not fault-tolerant.

2.2.2 Three Level Vienna Type Boost PFC Rectifier

The circuit topology of six-switch three-level Vienna type rectifier [4] is shown in Fig 2.2. This topology is well suited for aircraft applications. This converter is operated in continuous conduction mode.

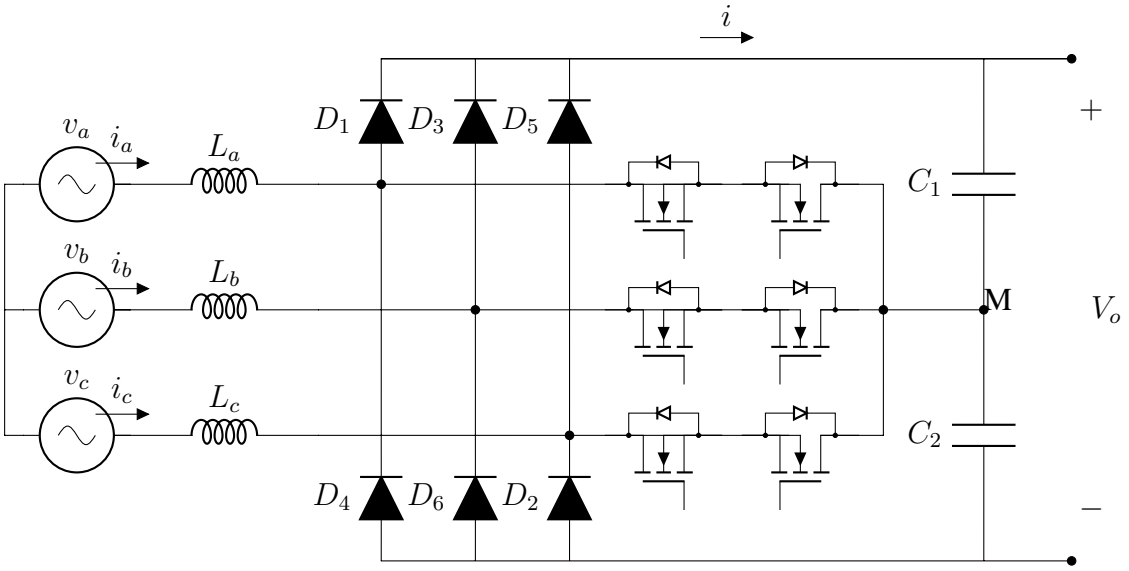

Figure 2.2: Three level Vienna Rectifier

2.2.3 Three Phase Delta Switch Boost Rectifier

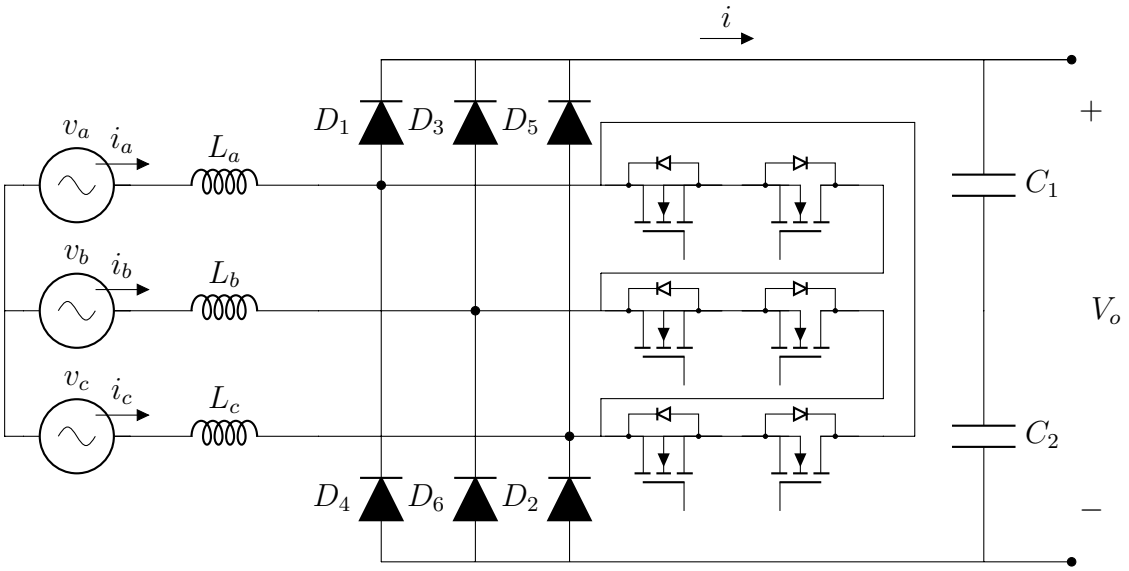

Figure 2.3: Three Phase Delta Switch Rectifier

Fig 2.3 shows the Three-phase delta switch rectifier [5] it is just a modification of Vienna rectifier where switches are connected in Delta configuration.

Main features:

- Reduced voltage stress across switches (Half the voltage stress in six switch boost converter).
- It has lower input mains current ripple resulting in reduced input inductance.
- Short circuit of DC bus because of the faulty control of semiconductor switches is not an issue in both the topologies so fault-tolerant which increases the reliability.

In general, the Y-connected switch realization shows higher conduction losses as compared to the Δ-connection, since there are always two (bidirectional) switches connected in series. Due to its low complexity, low conduction losses, and high reliability the Δ-switch rectifier topology seems to be an optimal choice for the realization of a rectifier for aerospace applications. Both the above topologies are operated in continuous conduction mode.

2.3 CCM Vs DCM

All the above mentioned PFC converter topologies are operated in continuous conduction mode (CCM) require two control loops; one is to regulate the output voltage and the other is to shape the input current sinusoidal. Hence the control strategy requires atleast five sensors (two input voltages, two input currents, One output voltage) for its implementation.

By reducing the number of sensors there are several advantages like cost reduction, improvement in system reliability, reduction of system weight, robustness to high-frequency noise, and a slight improvement in efficiency. For reducing the sensor count several approaches are reported in the literature for three-phase PFC AC-DC converters, where the system instability is the major concern during the load transients and also these control algorithms will not work in case of single-phase open faults.

The number of sensors in a converter can be reduced by operating the converter in a discontinuous conduction mode (DCM). A converter operating in DCM achieves

natural Power Factor Correction at the AC input side. Hence, there is no need for input current shaping circuits (i.e, inner current loop) therefore two input current and two input voltage sensors can be also eliminated.

In DCM, the average value of input current in a switching cycle is determined by the input voltage, which means the average input current naturally follows the input voltage.

In literature, several converter topologies are proposed operating in discontinuous conduction mode for reducing sensor count in Boost and Buck-Boost topologies. But in boost type topologies input current waveforms are distorted and consist of higher amplitude lower order harmonics. Therefore to filter out these lower-order harmonics large size input filters are required resulting in low power density.

On the other hand, the discontinuous mode Buck-Boost type converters are perfect PFC converters and the input current does not contain any lower order harmonics, hence a small input filter is sufficient to filter out the higher amplitude lower order harmonics. Some of the DCM operated Buck-Boost topologies are discussed in further chapters.

CHAPTER 3

Three Phase Buck-Boost Derived PFC converter

The three-phase buck-boost derived PFC converter [6] is operated in discontinuous conduction mode for more electric aircraft applications with reduced switching, sensing, and control requirements. Fig 3.1 shows the circuit topology consists of an input filter, three switches at input AC side, Diode bridge, and three input inductors connected in Δ-configuration. The converter is operated in DCM which eliminates the inner current loop and it further decreases the sensor count. It requires only one output voltage sensor, unlike five sensors in the PFC converter for control implementation. A simple voltage control loop is used to generate gate signals.

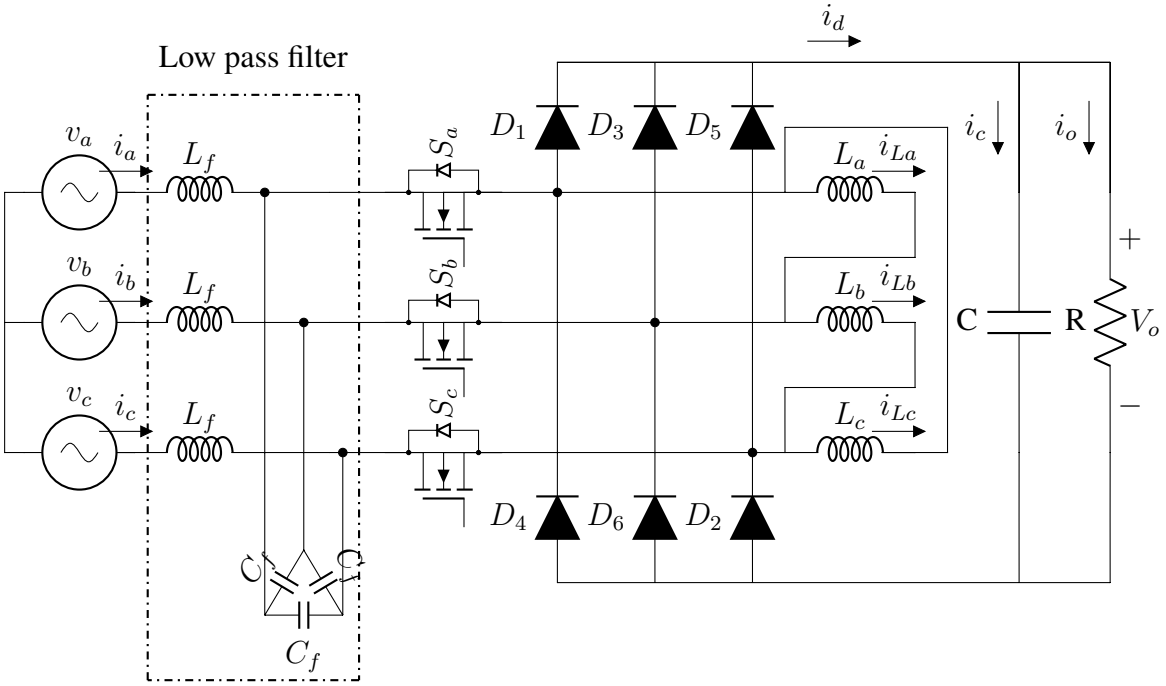

Figure 3.1: Three phase Buck-Boost derived PFC converter with inductors connected in Δ-configuration

All three switches are operated synchronously. The input inductors are connected in Δ-configuration, as it results in 20% less the peak inductor current when compared to the Y-configuration. Moreover, in case of a single-phase failure or open switch fault, all the inductors participate for power transfer.

3.1 Objectives

The main objectives of PFC converters are:

1. Input current should be sinusoidal and in phase with the voltage.
2. Regulated DC output voltage.

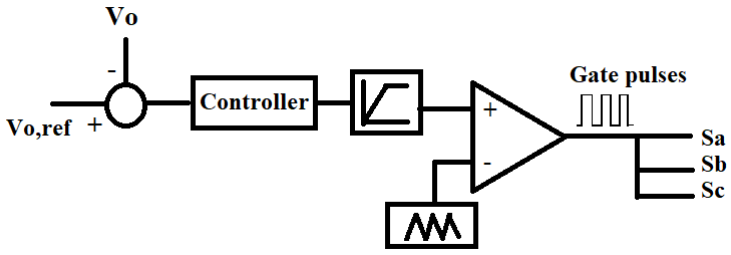

Figure 3.2: Voltage control circuit of the Converter

The first objective is achieved by operating the inductors in DCM. In DCM, the average value of input current in a switching cycle is determined by the input voltage, which means the average input current naturally follows the input voltage.

The second objective is achieved by using a simple voltage control loop as shown in Fig 3.2, It is considered that all the switches are operated synchronously and the value of input inductance in each phase is the same. From the voltage control loop shown in Fig 3.2, it can be seen that the duty cycle of the switches depends only on the error between the reference voltage and the output voltage i.e., for a given output power and input voltage, the converter duty cycle is constant and it does not change with input voltage sinusoidal variation. Duty cycle changes only when there is a change in output voltage reference or disturbances like load variation or any input voltage amplitude variation.

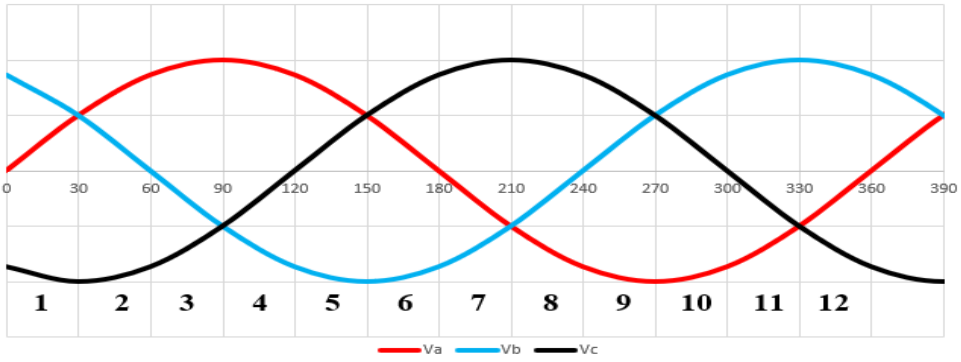

Figure 3.3: Three phase sinusoidal input voltages

For the analysis, three-phase sinusoidal signals are divided into 12 sectors of each 30° as shown in Fig 3.3. Due to the symmetric nature of the converter, its behavior is the same in each sector. Hence, the analysis is presented only for sector-1 i.e., for ωt = 0 to $\frac{\pi}{6}$. The three-phase input inductor current waveforms of the converter for one switching cycle operating in DCM in sector-1 are shown in Fig 3.4. It is observed that the converter has four operating modes in one switching cycle.

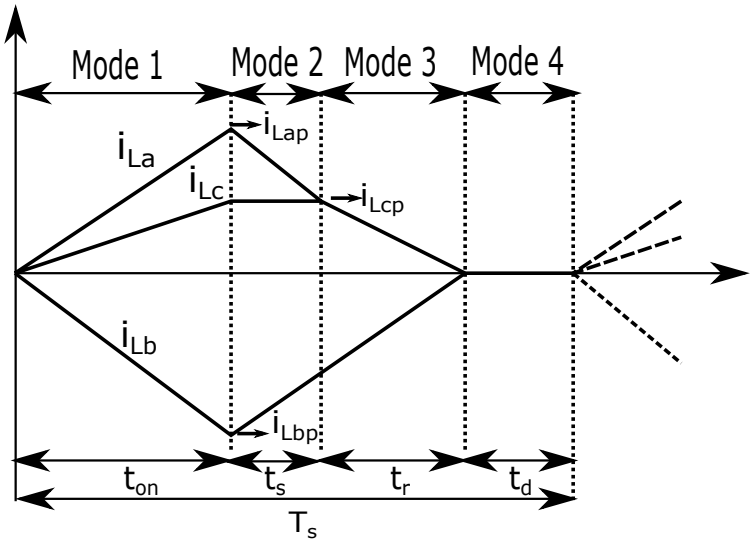

Figure 3.4: Input inductor currents in sector-1

When all the three switches (MOSFET's) are ON at once Line voltages v_{ab}, v_{bc}, v_{ca} will fall across input inductors L_a, L_b, L_c. Consequently, inductor currents i_{La}, i_{Lb}, i_{Lc} begin simultaneously to rise from zero at a rate proportional to instantaneous values of their respective line voltages. The specific inductor peak current values during each ON interval are proportional to the average values of their input line voltages during the same ON interval. Since each of these input line voltage average values varies sinusoidally, the inductor current peak and average values also vary sinusoidally. Subsequently, the line currents i_a, i_b, i_c average values also vary sinusoidally. The LC filter placed at the input side eliminates high-frequency components and only fundamental is present in the input currents at mains which are sinusoidal and in phase with the phase voltages.

3.2 Modes of Operation

3.2.1 Mode-1

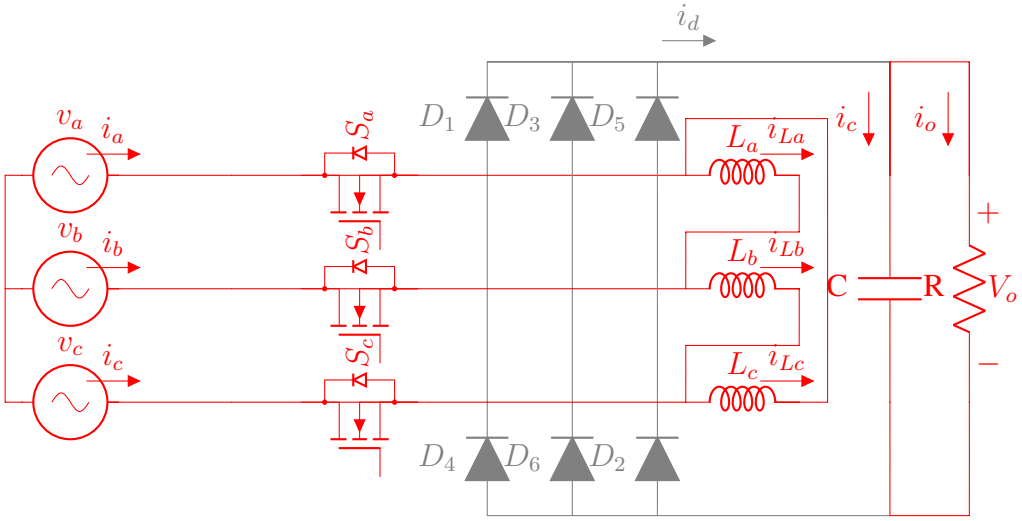

Figure 3.5: Equivalent circuit operation of Mode-1

In the first mode of operation all switches S_a, S_b, S_c are ON simultaneously. Prior to this mode all the input inductors L_a, L_b, L_c are in demagnetised state,so all the three switches turn ON with zero current. The equivalent circuit for this mode is shown in Fig 3.5, In this mode, output voltage is greater than the peak line-line input voltage so no diode will conduct, input inductors store the energy according to input line voltages v_{ab}, v_{bc}, v_{ca} that appear across the inductors L_a, L_b, L_c respectively. During this mode output capacitor will supply the load current. At the end of this mode inductor currents i_{La}, i_{Lb}, i_{Lc} will reach to their peak values as shown in Fig 3.4.

3.2.2 Mode-2

This mode starts when gating signals for the three switches are withdrawn.The equivalent circuit of the converter in this mode is shown in Fig 3.6. Inductors L_a, L_b starts discharging by giving stored energy to load through diodes D_2, D_3, D_4 at the rate of $\frac{V_o}{L}$. Inductor L_c retains its peak value (as L_c is shorted). This mode ends when Inductor current of L_a equal to peak inductor current of L_c i.e., $i_{La} = i_{Lcp}$ as shown in Fig 3.4.

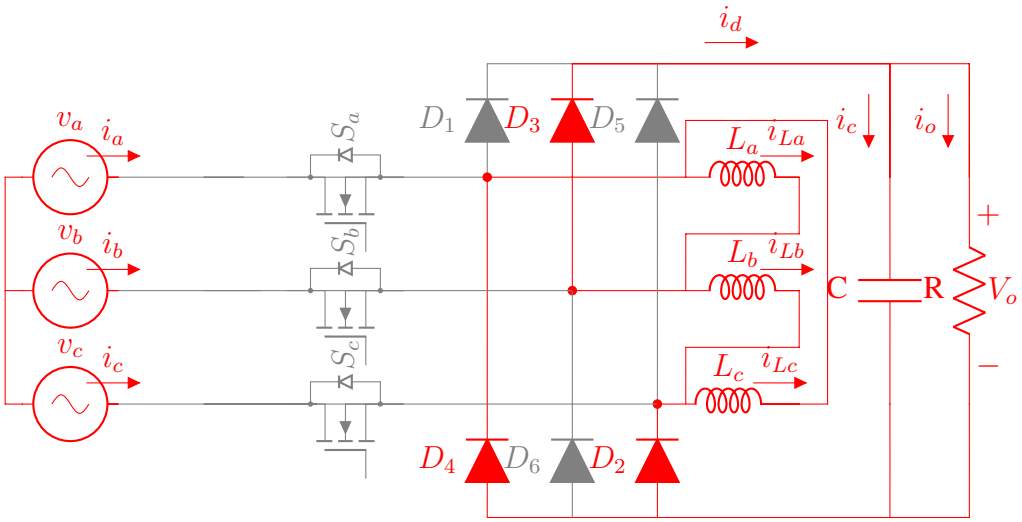

Figure 3.6: Equivalent circuit operation of Mode-2

3.2.3 Mode-3

The equivalent circuit of the converter in this mode is shown below. In this mode, all three inductors L_a, L_b, L_c start to reset by giving the stored energy to the load through diodes D_2, D_3 at a rate of $\frac{Vo}{2L}$, $\frac{Vo}{L}$, $\frac{Vo}{2L}$ respectively. This mode ends when all the inductors currents reach zero as shown in Fig 3.4.

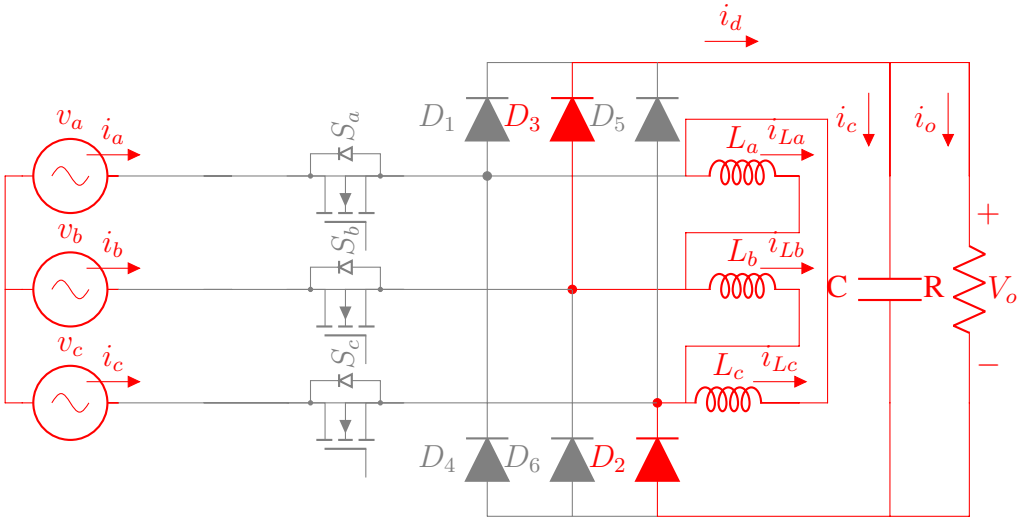

Figure 3.7: Equivalent circuit operation of Mode-3

3.2.4 Mode-4

The equivalent circuit of the converter in this mode is shown below. In this mode, all the input inductors are fully demagnetized and all the switches, diodes are in OFF state. The output filter capacitor supplies the load. This mode continues till the next switching period starts.

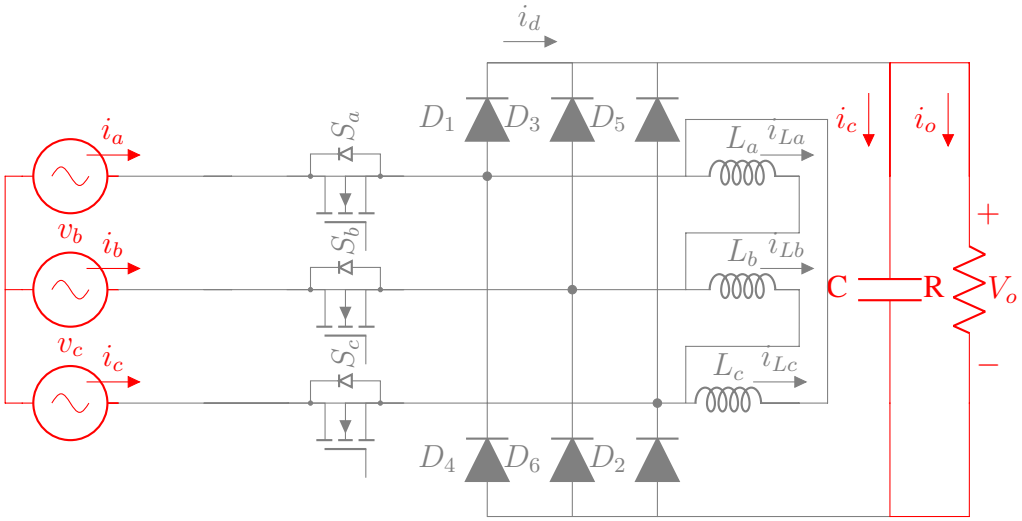

Figure 3.8: Equivalent circuit operation of Mode-4

3.3 Steady State Analysis and Design Calculations

In the analysis some of the following assumptions are made:

1. All the switches, inductors, and capacitors are ideal.
2. The output filter is large enough to maintain the output voltage constant.
3. As switching frequency is much higher than line frequency, the phase voltages and output voltage are assumed constant in one switching cycle.
4. The input inductor values in each phase are same

$$L_a = L_b = L_c = L. \tag{3.1}$$

According to the modes of operation, the input inductor current equations are defined and tabulated in Table 3.1.

Table 3.1: Mathematical representation of three phase inductor currents for different modes of operation in sector-1

Description	**Mode-1**	**Mode-2**	**Mode-3**	**Mode-4**
$i_{La}(t)$	$i_{La}(t) = \frac{v_{ab}}{L}t$	$i_{La}(t) = I_{Lap} - \frac{V_o}{L}t$ $i_{Lap} = \frac{v_{ab}}{L}t_{on}$	$i_{La}(t) = I_{Las} - \frac{V_o}{2L}t$ $I_{Las} = \frac{v_{ca}}{L}t_{on}$	$i_{La}(t) = 0$
$i_{Lb}(t)$	$i_{Lb}(t) = \frac{v_{bc}}{L}t$	$i_{Lb}(t) = I_{Lbp} - \frac{V_o}{L}t$ $i_{Lbp} = \frac{v_{bc}}{L}t_{on}$	$i_{Lb}(t) = I_{Lbs} + \frac{V_o}{L}t$ $I_{Lbs} = -\frac{2v_{ca}}{L}t_{on}$	$i_{Lb}(t) = 0$
$i_{Lc}(t)$	$i_{Lc}(t) = \frac{v_{ca}}{L}t$	$i_{Lc}(t) = I_{Lcp}$ $i_{Lcp} = \frac{v_{ca}}{L}t_{on}$	$i_{Lc}(t) = I_{Lcs} - \frac{V_o}{2L}t$ $I_{Las} = \frac{v_{ca}}{L}t_{on}$	$i_{Lc}(t) = 0$
Time period	t_{on}= DT_S	$t_s = \frac{3v_a}{V_o}DT_S$	$t_r = \frac{2v_{ca}}{V_o}DT_S$	t_d= T_S-t_{on}-t_s-t_r

*where D = Duty cycle of the switch and T_S = Switching period

3.4 Discontinuous Mode of Operation

To operate the converter in Discontinuous mode of operation, it should satisfy the following condition from Fig 3.4.

$$t_{on} + t_s + t_r \leq T_S \tag{3.2}$$

$$DT_S + \frac{3v_a}{V_o}DT_S + \frac{2v_{ca}}{V_o}DT_S \leq T_S$$

$$D\left[1 + \frac{3v_a}{V_o} + \frac{2v_{ca}}{V_o})\right] \leq 1$$

$$D\left[1 + \frac{3v_a}{V_o} + \frac{2v_c - 2v_a)}{V_o})\right] \leq 1$$

$$D\left[1 + \frac{v_a}{V_o} + \frac{2v_c}{V_o})\right] \leq 1$$

$$D\left[1+\frac{v_m sinwt}{V_o}+\frac{2v_m sin(wt+120)}{V_o})\right]\leq 1$$

$$D\left[1+\frac{sinwt}{M}+\frac{2sin(wt+120)}{M})\right]\leq 1$$

$$where \quad M=\frac{V_o}{v_m}$$

$$D\left[\frac{M+sinwt+2sin(wt+120)}{M}\right]\leq 1$$

$$D\left[\frac{M+sinwt+2\left[sin(wt)cos(120)+cos(wt)sin(120]\right)}{M}\right]\leq 1$$

$$D\left[\frac{M+\sqrt{3}coswt}{M}\right]\leq 1$$

$$D\leq\left[\frac{M}{M+coswt\sqrt{3}}\right]$$

$$D\leq\left[\frac{M}{M+\sqrt{3}sin(wt+90)}\right] \tag{3.3}$$

when $sin(wt+90)=1$ then $wt=0$ therefore to operate in DCM

$$D\leq\frac{M}{M+\sqrt{3}} \tag{3.4}$$

$$where \quad M=\frac{V_o}{v_m}$$

The critical value of voltage conversion ratio(M) defines the boundary between the continuous mode and discontinuous mode and given by the equation.

$$M_{cr}=\frac{\sqrt{3}D}{1-D} \tag{3.5}$$

In this PFC converter, the output voltage should be higher than the peak line-to-line voltage to ensure the reverse bias of bridge diodes D1 to D6 . Hence, for a given duty cycle D, the converter is said to be operated in DCM when $M\geq M_{cr}\geq\sqrt{3}$

3.5 Average Output Current

In a switching cycle, the average current of the output filter capacitor is zero. Therefore, for the sector under the analysis $(0 - \frac{\pi}{6})$, the average output current of the converter is same as the average current of diode D_3 given by

$$i_{o,avg} = \langle i_o \rangle = \langle i_{d3} \rangle \tag{3.6}$$

equation of $i_{d3}(t)$ in Mode-2 is given by

$$i_{d3}(t) = i_{La}(t) - i_{Lb}(t)$$

$$i_{d3}(t) = \frac{-3v_b}{L} DT_S - \frac{2v_o}{L} t \tag{3.7}$$

equation of $i_{d3}(t)$ in Mode-3 is given by

$$i_{d3}(t) = \frac{3v_{ca}}{L} DT_S - \frac{3v_o}{2L} t \tag{3.8}$$

From equations (3.7) and (3.8) average value of output current in a switching cycle can be calculated by integrating over a switching period

$$i_{o,avg} = \frac{1}{T_s} \left[\int_{DT_s}^{t_s+DTs} \left(\frac{-3v_b}{L} DT_S - \frac{2v_o}{L} t \right) dt + \int_{t_s}^{t_r+t_s} \left(\frac{3v_{ca}}{L} DT_S - \frac{3v_o}{2L} t \right) dt \right]$$

Therefore average value of output current in switching cycle is given by

$$i_{o,avg} = \langle i_{d3} \rangle = \frac{9D^2 T_s V_m^2}{4LV_o} \tag{3.9}$$

The average output current in a line period is given by

$$I_{o,avg} = \frac{6}{\Pi} \int_0^{\frac{\Pi}{6}} i_{o,avg} d(wt)$$

$$I_{o,avg} = \frac{6}{\Pi} \int_0^{\frac{\Pi}{6}} \frac{9D^2 T_s V_m^2}{4LV_o} d(wt) \tag{3.10}$$

$$I_{o,avg} = \frac{9D^2T_sV_m^2}{4LV_o} \tag{3.11}$$

3.6 Input Current

The expression for input phase-a current before filtering is

$$i_a(t) = \frac{3v_a}{L}t \qquad for \qquad 0 \leq t \leq t_{on} \tag{3.12}$$

$$= 0 \qquad for \qquad t_{on} \leq t \leq t_s \tag{3.13}$$

where $v_a = v_m sin(wt)$ taking Fourier series for input current over one switching cycle.

$$i_a(t) = \frac{a_0}{2} + \sum_{n=1}^{\infty}(a_n cos(nw_s t) + b_n sin(nw_s t)) \tag{3.14}$$

where

$$a_o = \frac{3v_aD^2T_s}{L}$$

$$a_h = \frac{6v_a}{nw_sL}\left((Dsin(2nD\pi)) + \frac{1}{2n\pi}cos(2nD\pi) - \frac{1}{2n\pi}\right)$$

$$b_h = \frac{6v_a}{nw_sL}\left(\frac{1}{2n\pi}sin(2nD\pi) - Dcos(2nD\pi)\right)$$

On combining harmonic components and substituting $v_a = V_m sin(wt)$ we get

$$i_a(wt) = \frac{3V_mD^2T_s}{L}sin(wt) + \sum_{n=1}^{\infty}\frac{6V_mD}{nw_sL}sin(wt)sin(nw_st + \delta_n) \tag{3.15}$$

where $\delta_n = \tan^1(\frac{b_h}{a_h})$

The first term in the equation (3.15) represents fundamental components and second term represent the harmonic component in the input current i_a . By designing the low pass LC filter with cut off frequency much lower tan the switching frequency the harmonic components can be eliminated therefore resulting input current containing only fundamental component

$$i_a(wt) = \frac{3V_mD^2T_s}{L}sin(wt) = I_m sin(wt) \tag{3.16}$$

$$I_m = \frac{3V_m D^2 T_s}{L} \tag{3.17}$$

Equation (3.16) shows that input phase-A current is sinusoidal and in phase with the input voltage. which proves the unity power factor operation of the converter.

3.7 Input Inductor Design

The input inductor design is to be such that it has to maintain the DCM for minimum input voltage and maximum output power (rated power) condition. Because at this condition, the converter input current is maximum, and consequently the inductor current peak also will be maximum. If the inductor can demagnetize within a switching period at this condition, then the DCM would be ensured for all the input voltages above the minimum input voltage and for all the output powers below rated power.

Therefore by using equation (3.4) maximum duty cycle D_{max} which ensure the DCM operation for minimum input voltage can be given as

$$D_{max} \leq \frac{V_o}{V_o + \sqrt{3}Vm, min} \qquad since \quad M = \frac{V_o}{V_m} \tag{3.18}$$

The average output current for the given rated power and the rated output voltage is expressed as

$$I_o = \frac{P_o}{V_o} \tag{3.19}$$

from equations (3.11), and (3.19)

$$\frac{P_o}{V_o} = \frac{9D_{max}^2 T_s V_m^2}{4LV_o} \tag{3.20}$$

From the above equation The value of the input inductor to operate the converter always in DCM is given as

$$L \leq \frac{9D_{max}^2 T_s V_{m,min}^2}{4P_o} \tag{3.21}$$

3.8 Modelling of Converter

The small signal model of the converter is obtained by using current injected equivalent circuit approach [7]. In this approach, the non-linear part of the circuit is linearised by injecting the average output current in a switching cycle i.e $i_{o,avg}$ produced by the non-linear part of the circuit into the linear part as shown in below Figure

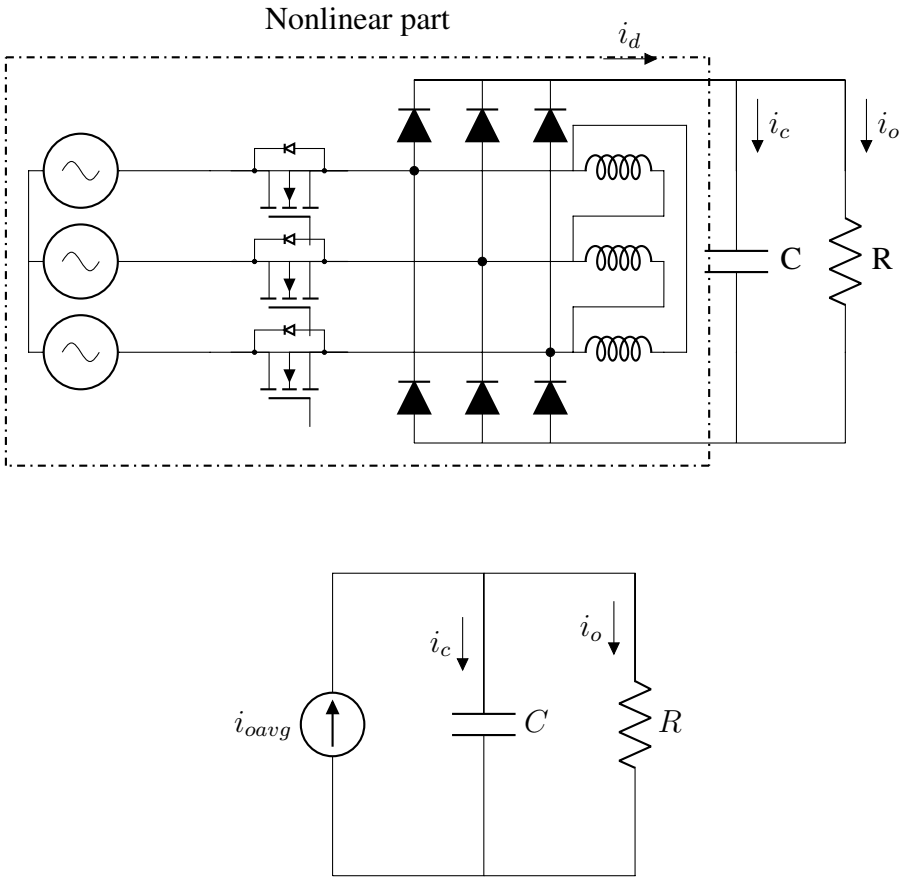

Figure 3.9: Equivalent circuit of the converter for small-signal modeling

On applying the small signal perturbations to equations (3.11) and (3.17) around steady state operating point making small signal approximations.

$$I_{o,avg} = \frac{9D^2T_sV_m^2}{4LV_o}$$

$$(I_o + \hat{i_o}) = \frac{9(D+\hat{d})^2T_s(V_m+\hat{v_m})^2}{4L(V_o+\hat{v_o})}$$

$$(I_o + \hat{i_o}) = \frac{9(D^2+(\hat{d})^2+2D\hat{d})T_s((V_m)^2+(\hat{v_m})^2+2V_m\hat{v_m})}{4L(V_o+\hat{v_o})}$$

By separating steady state terms and small signal terms

we have

$$\hat{i_o} = \frac{9DT_sV_m^2}{4Lv_o}\hat{d} + \frac{9D^2T_sV_m}{4Lv_o}\hat{v_m}$$

$$\hat{i_o} = j_2\hat{d} + g_2\hat{v_m} - \frac{1}{r_2}\hat{v_o} \tag{3.22}$$

$$j_2 = \frac{9DT_sV_m^2}{4Lv_o} \qquad g_2 = \frac{9D^2T_sV_m}{4Lv_o} \qquad r_2 = \frac{V_o}{i_{o,avg}}$$

On applying small signal perturbations to equation (3.17)

$$I_m = \frac{3V_mD^2T_s}{L}$$

$$(I_m + \hat{i_m}) = \frac{3(V_m + \hat{v_m})(D + \hat{d})^2T_s}{L}$$

$$(I_m + \hat{i_m}) = \frac{3V_mD^2T_s}{L} + \frac{3V_mDT_s}{L}\hat{d} + \frac{3D^2T_s}{2L}\hat{v_m}$$

$$\hat{i_m} = j_1\hat{d} + \frac{1}{r_1}\hat{v_m} \tag{3.23}$$

$$j_1 = \frac{3V_mDT_s}{L} \qquad r_1 = \frac{3D^2T_s}{2L}\hat{v_m}$$

$$\hat{i_o} = j_2\hat{d} + g_2\hat{v_m} - \frac{1}{r_2}\hat{v_o}$$

$$\hat{i_m} = j_1\hat{d} + \frac{1}{r_1}\hat{v_m}$$

Fig 3.10 shows the equivalent small signal model representation of the derived buck-boost converter by using equations (3.22) and (3.23)

From Fig 3.10, considering resistive load R

$$\hat{i}_{o,avg} = \hat{v}_o\left(\frac{1}{R} + \frac{1}{X_c}\right)$$

$$\hat{i_o} = j_2\hat{d} + g_2\hat{v_m} - \frac{1}{r_2}\hat{v_o}$$

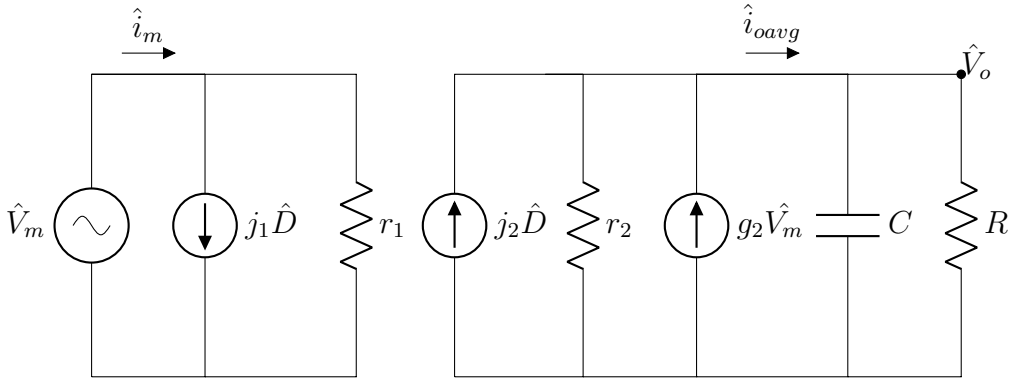

Figure 3.10: Small signal model equivalent circuit

Applying laplace to above equation, considered variation of $\hat{i}_{o,avg}$ w.r.t $\hat{v}_m$ is zero

$$\hat{i_o}(s) = j_2\hat{d}(s) - \frac{1}{r_2}\hat{v}_o(s)$$

$$\hat{i}_o(s) = \left(\frac{1}{R} + sC\right)\hat{v}_o(s) \qquad r_2 = \frac{V_o}{I_o}$$

$$\hat{i_o}(s) = j_2\hat{d}(s) - \frac{1}{r_2}\hat{v}_o(s)$$

$$\hat{v}_o(s)\left(\frac{1}{R} + sC + \frac{I_o}{V_o}\right) = j_2\hat{d}(s)$$

$$\frac{\hat{v}_o(s)}{\hat{d}(s)} = \frac{j_2}{\left(\frac{1}{R} + sC + \frac{I_o}{V_o}\right)}$$

Substituting j_2 and I_o in the above equation we have

$$\frac{\hat{v}_o(s)}{\hat{d}(s)} = \frac{\frac{9DT_sV_m^2R}{2LV_o}}{1 + \frac{9D^2T_sV_m^2R}{4LV_o^2} + sRC} \tag{3.24}$$

Similarly applying small signal perturbations to the equation (3.17) around the steady state operating point considering small signal approximations

$$\hat{i_m} = j_1\hat{d} + \frac{1}{r_1}\hat{v_m}$$

$$\frac{\hat{v}_o(s)}{\hat{v_m}(s)} = \frac{\frac{9D^2T_sV_m^2R}{2LV_o}}{1 + \frac{9D^2T_sV_m^2R}{4LV_o^2} + sRC} \tag{3.25}$$

By considering Resistive load, transfer functions of output voltage to duty ratio and output voltage to input voltage are obtained

$$\frac{\hat{v}_o(s)}{\hat{d}(s)} = \frac{2V_m K}{1 + \frac{KV_m D}{V_o} + sRC} \tag{3.26}$$

$$\frac{\hat{v}_o(s)}{\hat{v_m}(s)} = \frac{2KD}{1 + \frac{KV_m D}{V_o} + sRC} \tag{3.27}$$

where

$$K = \frac{9DT_s V_m R}{4LV_o}$$

In this chapter, a three-phase buck-boost PFC converter with inductors connected in Δ- configuration is presented. A detailed analysis of the operating modes, steady-state analysis, design parameters ensuring DCM operation is discussed. A small-signal model is obtained using current injected equivalent circuit approach and transfer functions of the converter are derived.

CHAPTER 4

Control Design of Three Phase Buck-Boost Derived PFC Converter

In this chapter, design parameters are calculated for the following specifications for the three-phase buck-boost PFC converter. As the converter is operated in DCM to achieve PFC at AC input, the converter control is quite simple and requires only one simple voltage control loop to regulate the output voltage, as the inner current control loop is eliminated. The small-signal model of the converter is derived by using the current injected equivalent circuit approach (CIECA) to aid the controller design. A simple PI controller is designed in this chapter for allowing the voltage loop bandwidth of 210 rad/sec with phase margin(P.M) 86° and infinite gain margin [8].

Table 4.1: Input specifications of PFC converter

Parameter	**Value**
Line-Line voltage, V_{LLrms}	110V $\pm$ 15%
Input frequency, f	400Hz
Output power, P_o	2kW
Output voltage, V_o	270V
Switching frequency, f_s	50kHz

4.1 Calculation of Design Parameters

4.1.1 Duty Ratio(D)

From the equation (3.18)

$$D_{max} \leq \frac{V_o}{V_o + \sqrt{3}Vm, min}$$

$$V_o = 270$$

$$V_m = 110\frac{\sqrt{2}}{3} = 89.81V$$

$$V_m = 89.81 \pm 15\%$$

$$V_{m,min} = 76.34V \qquad V_{m,max} = 103.28V$$

$$D_{max} \leq \frac{270}{270 + \sqrt{3}(76.34)}$$

$$D_{max} \leq 0.78$$

$D = 0.6$ is considered for the simulation

4.1.2 Input Inductance

From equation (3.21)

$$L \leq \frac{9D_{max}^2 T_s V_{m,min}^2}{4P_o}$$

Substituting all the variables in the above equation we have the maximum inductance value required to operate the converter always in DCM i.e

$$L \leq 79.78uH$$

$L = 65uH$ chosen for simulation

4.1.3 Load Resistance

Considering Resistive load

$$P_o = \frac{V_o^2}{R}$$

$$R = \frac{270^2}{2000} = 36.45$$

4.1.4 Voltage Loop Gain Transfer Function

From the equation (3.26) converter transfer function obtained is

$$G_{vd} = \frac{\hat{v}_o(s)}{\hat{d}(s)} = \frac{\frac{9DT_s V_m^2 R}{2LV_o}}{1 + \frac{9D^2 T_s V_m^2 R}{4LV_o^2} + sRC}$$

Substituting all the variables in the above transfer function we get

$$G_{vd} = \frac{\hat{v}_o(s)}{\hat{d}(s)} = \frac{904.2}{2 + 0.0164s} \tag{4.1}$$

4.1.5 Bode Plot For Voltage Loop Transfer Function

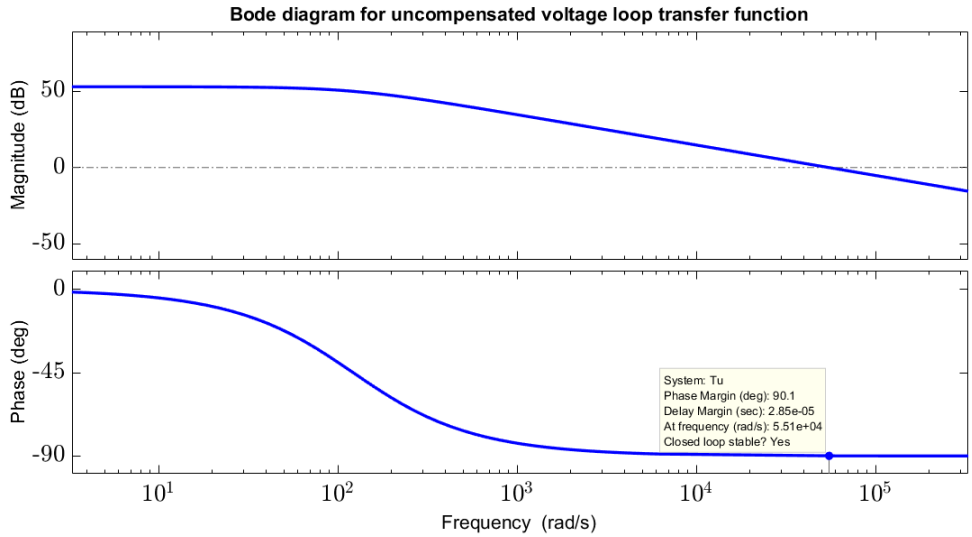

Figure 4.1: Bode plot of uncompensated voltage loop gain transfer function

A proportional-integral controller is designed for allowing the voltage loop bandwidth of 210 rad/sec with a phase margin (P.M) 86° and infinity gain margin. From the bode plot phase at 210 rad/sec is -58°

$$P.M = -58 + 180 = 122^\circ$$

$$P.M_{desired} = 86^\circ \qquad at \qquad 210 rad/sec$$

A Lag Compensator is required to add a phase lag of 36°

4.2 Controller Design

Lag Compensator transfer function is

$$G_{pi}(s) = K_{pi}\left[\frac{S + w_L}{S}\right]$$

$$-36 = -90 + tan^{-1}\left(\frac{200}{w_L}\right)$$

$$54 = tan^{-1}\left(\frac{200}{w_L}\right)$$

$$w_L = 145 rad/sec$$

Gain at 210 rad/sec is 47dB

$$20log(k) = 47$$

$$k = 223.87$$

$$|G_c| = |G_{vd}||G_{pi}|$$

Gain at the gain crossover frequency should be one

$$1 = 223.87\ K_{pi}\sqrt{\frac{w_L^2 + w_C^2}{w_C^2}}$$

where w_C is cut off frequency or Bandwidth

$$1 = 223.87 K_{pi}\sqrt{\frac{145^2 + 200^2}{200^2}}$$

$$1 = 223.87(K_{pi})1.2352$$

$$K_{pi} = 0.00363$$

Therefore lag compensator

$$G_{pi} = 0.00363\left[\frac{S + 145}{S}\right]$$

$$G_{pi} = 0.00363\left[1 + \frac{145}{S}\right]$$

$$G_{pi} = \left[0.00363 + \frac{0.52}{S}\right] \tag{4.2}$$

G_{pi} can be modelled as PI controller

$$G_{pi} = K_p + \frac{K_i}{S}$$

Therefore $K_p \; and \; K_i$ values are

$$K_p = 0.00363$$

$$K_i = 0.52$$

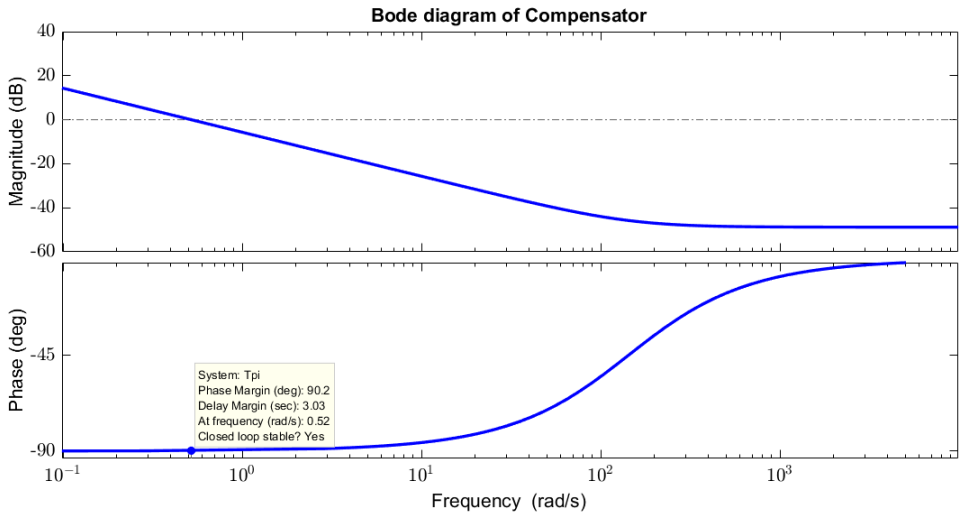

Figure 4.2: Bode plot of the compensater

The compensated loop gain transfer function is given by

$$G_{vd}G_{pi} = \left(\frac{904.2}{2 + 0.0164s}\right)\left(0.00363 + \frac{0.52}{S}\right) \tag{4.3}$$

From the bode plot in Fig 4.3, it is observed that required bandwidth of 210 rad/sec and Phase margin of 86° are obtained due to controller action. The loop gain transfer function described by equation (4.3) has -20 db slope at zero cross over frequency for all the loads below rated load. This indicates that the system is stable for all the load conditions.

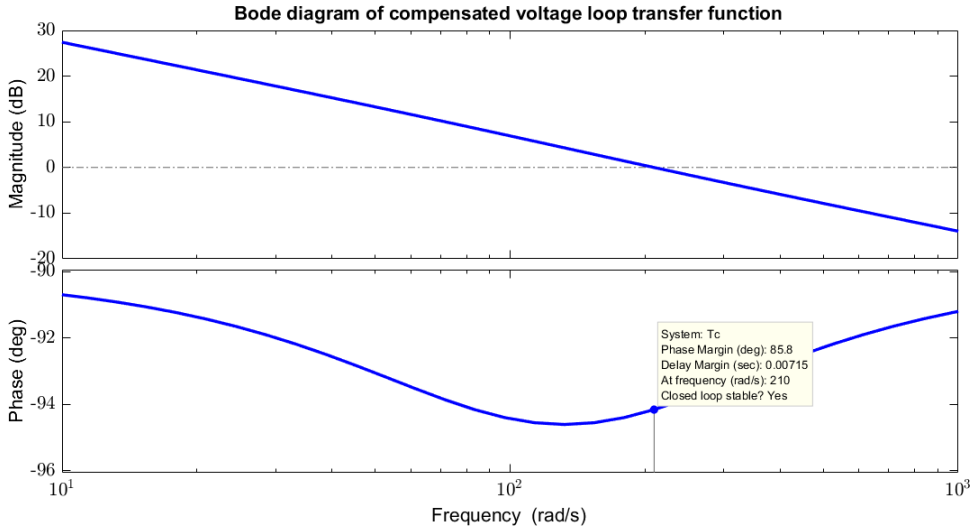

Figure 4.3: Bode plot of compensated voltage loop gain transfer function

Table 4.2: Design parameters

Parameter	**Value**
Maximum Duty cycle, D_{max}	0.78
Input inductor, L	$65\mu H$
Load resistance, R	36.45
Output capacitor, C	$450\mu F$
Duty cycle, D	0.6

In this chapter, simple PI controller for three-phase buck-boost derived PFC converter is designed for allowing the voltage loop bandwidth of 210 rad/sec with phase margin(P.M) 86° and infinite gain margin. The design parameters for ensuring the DCM operation of the converter are calculated.

CHAPTER 5

Simulation Study of Three Phase Buck-Boost Derived PFC Converter

A 2 kW, 400 Hz, 110 V AC RMS/270 V DC , three phase buck-boost PFC converter simulated in MATLAB/SIMULINK. Relevant waveforms showing the characteristics of the converter are presented.

5.1 Input Voltage and Input Current

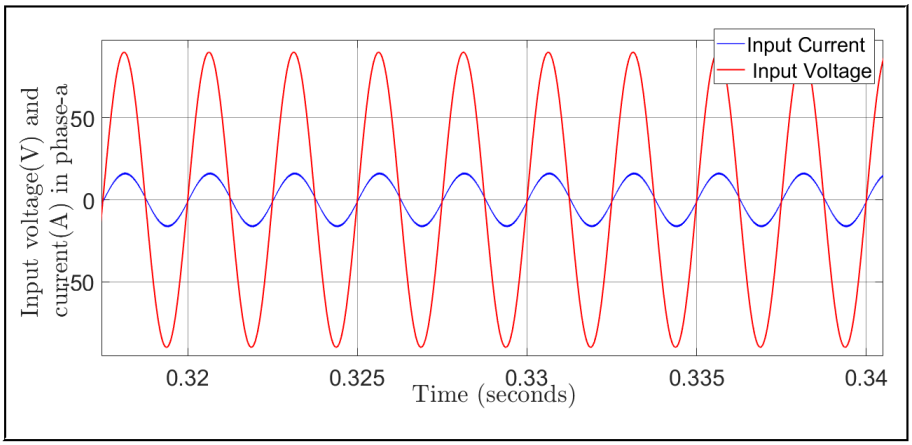

Figure 5.1: Input phase voltage and Input phase current of Phase-A

From the above Fig 5.1, it can be observed that input current $i_a(t)$ is sinusoidal and is in phase with the input voltage $v_a(t)$ of phase-a.

5.2 Three Phase Inductor Currents

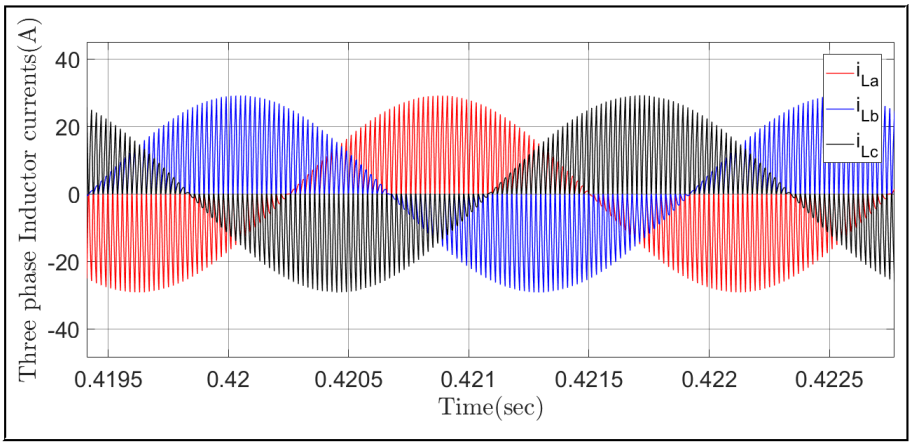

Figure 5.2: Input Inductor currents

When all the switches are ON, three inductors L_a, L_b, L_c come across the line voltages v_{ab}, v_{bc}, v_{ca} respectively. Consequently, the inductor currents i_{La}, i_{Lb}, i_{Lc} begin simultaneously to rise from zero at a rate proportional to the instantaneous values of their respective line voltages. The specific inductor peak current values during each ON interval are proportional to the average values of their input line voltages during the same ON interval. Since each of these line voltage average values vary sinusoidally, the inductor current peak and average values also vary sinusoidally as shown in Fig 5.2. Subsequently, the line currents i_a, i_b, i_c average values also vary sinusoidally.

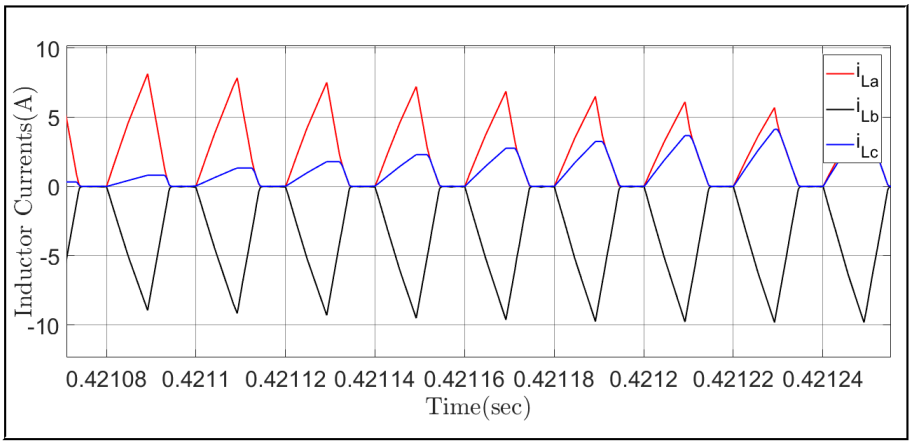

Figure 5.3: Inductor currents showing four modes of operation

Fig 5.3 shows the three phase input inductor currents operating four modes in sector-1 with charging, discharging and discontinuous conduction modes.

5.3 Current and Voltage Stress in Switch

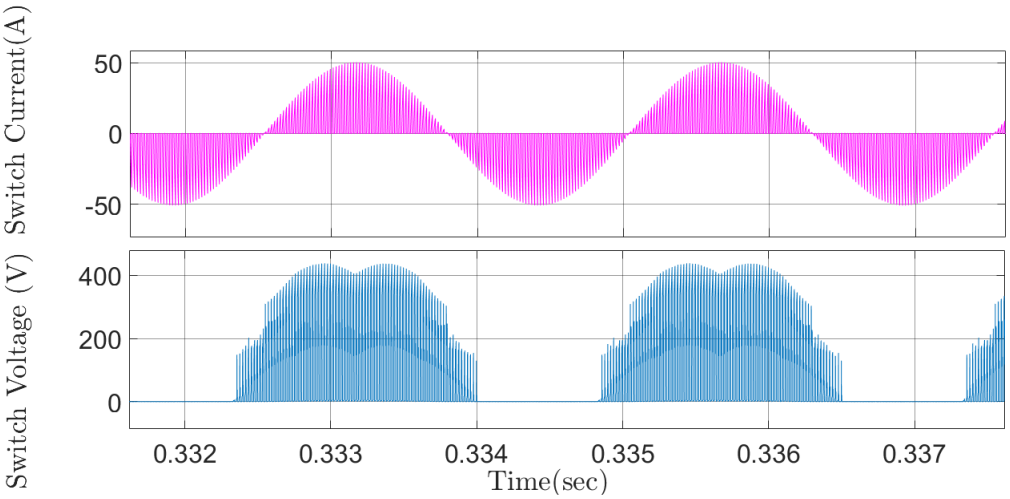

Figure 5.4: Switch Current and Voltage

Fig 5.4 shows the voltage across one of the power switch MOSFETs for a line cycle. In each phase, the body diode of the power switch which is in series with that the phase is forward biased for two-third of its negative cycle, when the phase negative amplitude is high. For example, the body diode of power switch S_a is forward biased from time t = 0.3325 to 0.3338 sec as shown in Fig 5.4 During this period, the other two power switch body diodes are reverse biased and experience a maximum voltage stress of peak line-to-line input voltage plus the output voltage. Hence, the maximum voltage across the power switch is given by

$$V_{sw,max} = \sqrt{3}V_m + V_o$$

5.4 Current and Voltage Stress in Diode

Fig 5.5, shows the voltage across the diode D_1 of full bridge rectifier for a line cycle. Each diode of the full-bridge rectifier experiences a maximum voltage stress of output voltage V_o, when the other diode in its phase leg is ON.

Voltage stress across the diode is

$$V_{D,max} = V_o$$

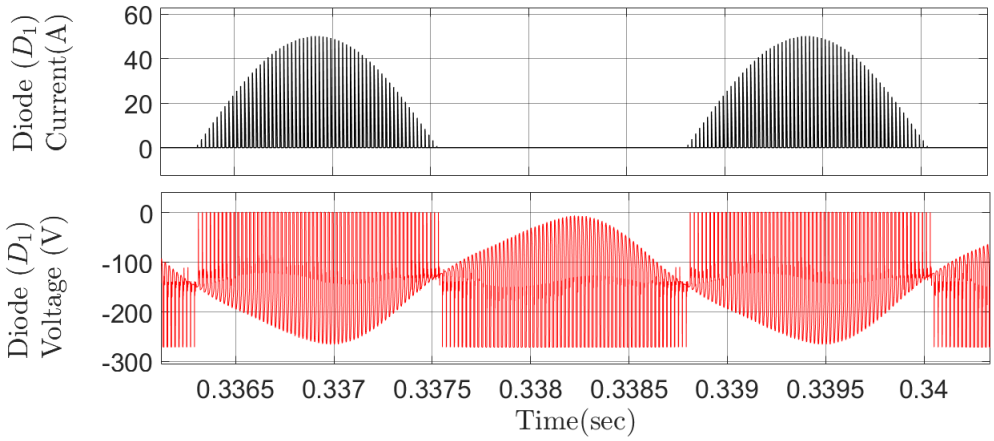

Figure 5.5: Diode Current and Voltage

5.5 Output Voltage

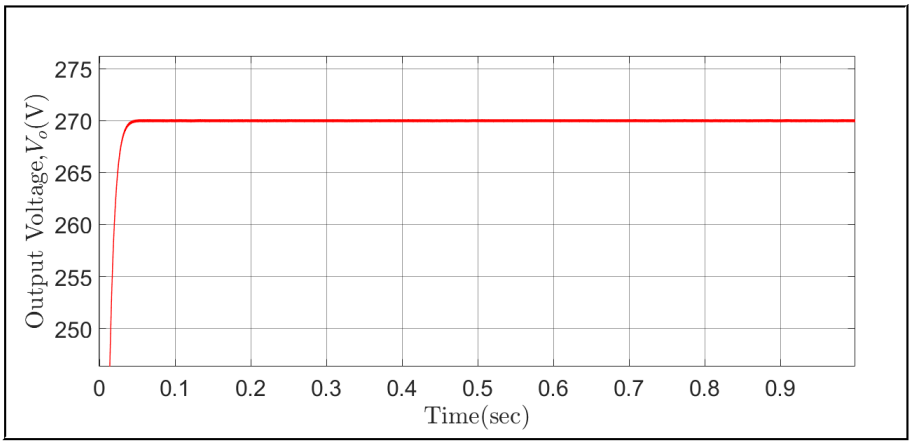

Figure 5.6: Output Voltage

The output voltage is settled at 270 V

5.6 Input Current THD

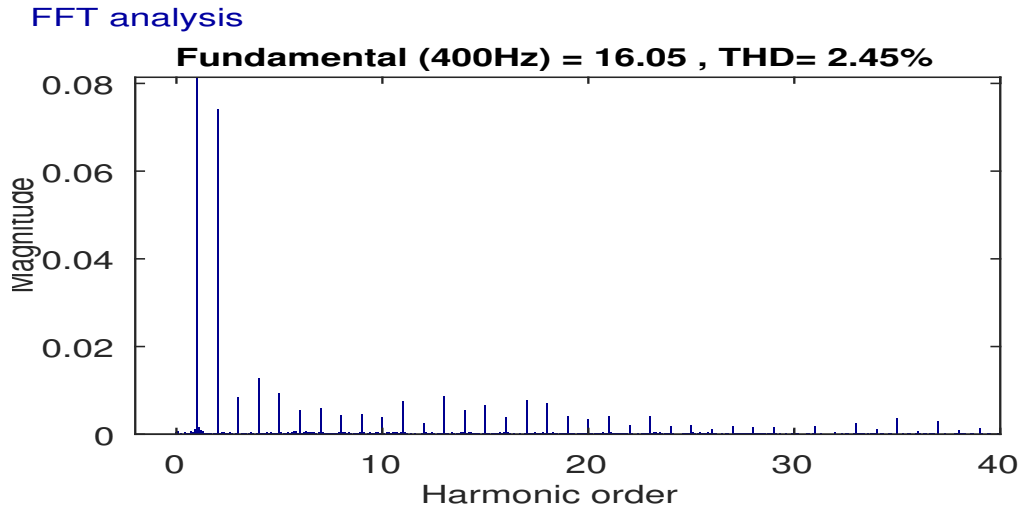

Figure 5.7: Input Current harmonic spectrum at 2 kW

According to the aircraft standard DO160F and military standard MILSTD704F , input current harmonics have stringent limitations and input current THD should be $< 5\%$. The individual input current harmonic limits are listed in TABLE 5.1.

Table 5.1: Current harmonics limits of three-phase equipment according to DO160F

Harmonic order	**Limits**I_n
$3^{rd}, 5^{th}, 7^{th}$	$0.02I_1$
Odd Triplen Harmonics ($9^{th}, 15^{th}, 21^{th}...39^{th}$)	$0.1I_1$/n
Odd Non-Triplen Harmonics ($11^{th}, 13^{th}$)	$0.03I_1$
Odd Non-Triplen Harmonics ($17^{th}, 19^{th}$)	$0.04I_1$
Odd Non-Triplen Harmonics ($23^{th}, 25^{th}$)	$0.03I_1$
Odd Non-Triplen Harmonics ($29^{th}, 31^{th}, 35^{th}, 37^{th}$)	$0.3I_1/n$
Even Harmonics ($2^{nd}, 4^{th}$)	$0.01I_1/n$
Even Harmonics>4 ($6^{th}, 8^{th}, 10^{th...}, 40^{th}$)	$0.0025I_1$

From Fig.5.7, it is verified that all the input current harmonics are with in the limits of aircraft standard DO160F mentioned in the table, and input current THD is 2.45%

CHAPTER 6

Three Phase Buck-Boost PFC Converter With Inductors in Y-Configurationn

Three-phase rectifier systems that offer power-factor correction(PFC) and a wide range of output voltages are often realized as combinations of two converter stages: AC - DC and DC-DC stages, the first stage ensures (PFC) sinusoidal input current and generate an intermediate DC voltage. The second one i.e DC-DC conversion stage is required to achieve a wide range of regulated DC output voltages. This two-stage approach is topologically complex and requires complicated control and modulation methods.

There are emerging applications such as more electric aircraft, where PFC functionality and also compatibility with widely varying AC to DC voltage ratios are required even for systems with low-power ratings ($< 1kW$). For such low-power rating systems, a two-stage approach is complex and costly. So single-stage three-phase buck-boost PFC converters are an interesting alternative.

These converters have capable of achieving sinusoidal input currents, a high power factor, a wide output voltage range, all with minimum control complexity when operated in DCM, i.e. without requiring any current sensors. Furthermore, these systems can continuously operate with a wide range of mains frequencies, e.g. in airborne applications.

6.1 State-of-the-art Topology

The state-of-the-art three-phase buck-boost PFC rectifier topology [9] shown in Fig 6.1 has been proposed by Pan and Chen already in 1994. However, topological variations are still in the scope of current research. From this base topology, three-phase buck-boost PFC converter with inductors in Δ-configuration (as discussed in Chapter 3) and Y-configuration are derived.

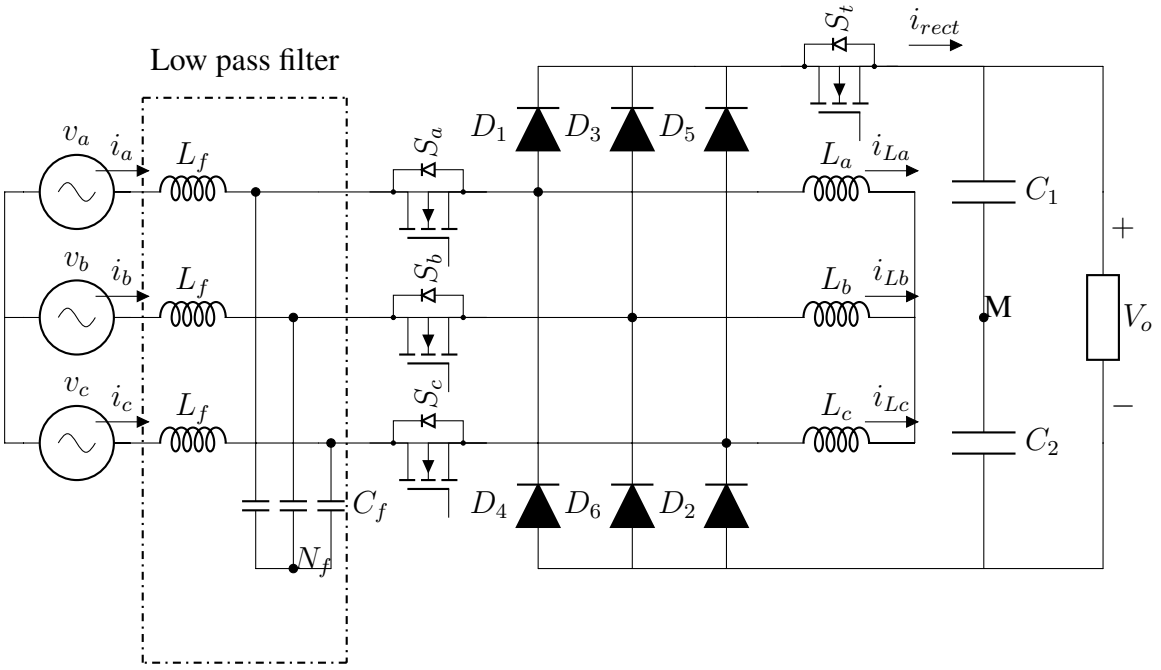

Figure 6.1: State-of-the-art buck–boost three-phase PFC rectifier

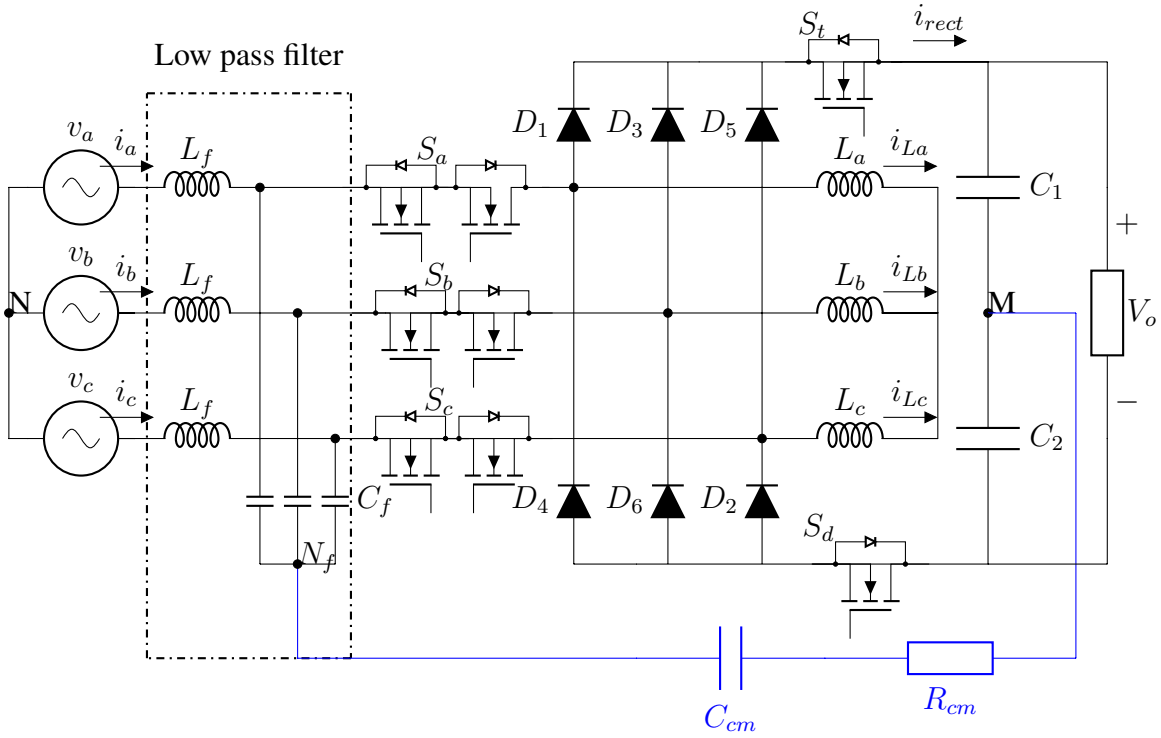

Figure 6.2: Extension to the State-of-the-art topology

6.2 Extension to the State-of-the-art Topology

The base topology shown in Fig 6.1 is extended [10] to mitigate three main issues: one is it allows the use of power semiconductors with lower blocking voltage ratings, as two switches connected in back to back are used so voltage that appears across each switch is reduced. The second one is, it provides the common-mode (CM) free output voltage. The third one is DC side switches (S_t, S_d) are used to isolate the AC mains from the output. The extended topology shown in Fig 6.2 retains the advantages simplicity of the original structure and control.

6.3 Modes of Operation

The basic operating principle of both three-phase buck-boost PFC rectifiers is essentially the same and will be briefly discussed. The simplicity of the system originates mainly by operating it in discontinuous conduction mode (DCM), i.e. the currents in the inductors L_a, L_b, and L_c are zero at the beginning of each switching period, and all switches are turned off.

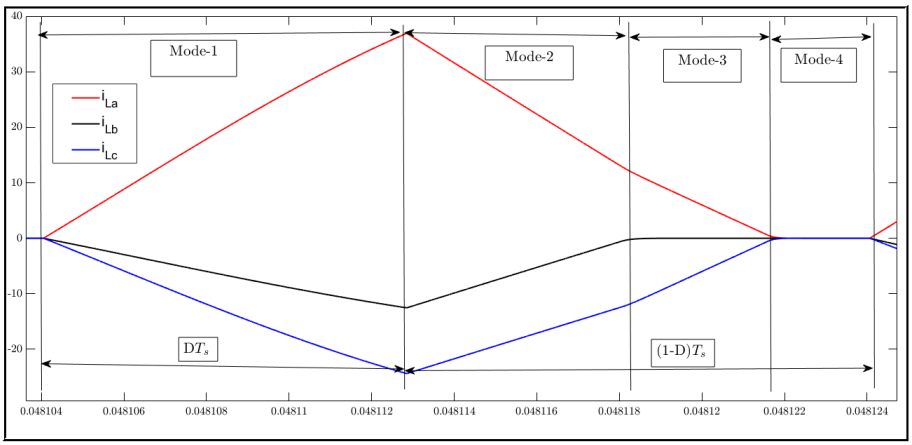

Figure 6.3: Four modes of Operation

6.3.1 Mode-1

During the first interval of a switching period, the AC-side switches S_a, S_b and S_c are turned on simultaneously, and hence the phase voltagesv_a, v_b, v_c are applied to the star-connected buck-boost inductors L_a, L_b and L_c. Starting from zero, the currents i_{La}, i_{Lb}, i_{Lc} change with a slope that is proportional to the corresponding phase voltages. No current flows through the diode bridge, regardless of the output voltage level, because the DC side is disconnected by the DC-side switches S_t, S_d or S_t in base topology. At the end of this magnetization interval, all AC-side switches are turned off simultaneously and the DC-side switch S_t (and S_b in case of the extended topology) are turned on. Note that the modulation signals are identical for all three phases, and a common duty cycle D is employed.

In state-of-art-topology as there is no bottom DC side switch (S_d), $v_c < 0$, diode D_2 will conduct so output is directly shorted to AC mains. This problem is solved by adding Switch(S_d) at the DC-side in the bottom. voltage appeared across the switch is S_t = v_a - $V_o/2$

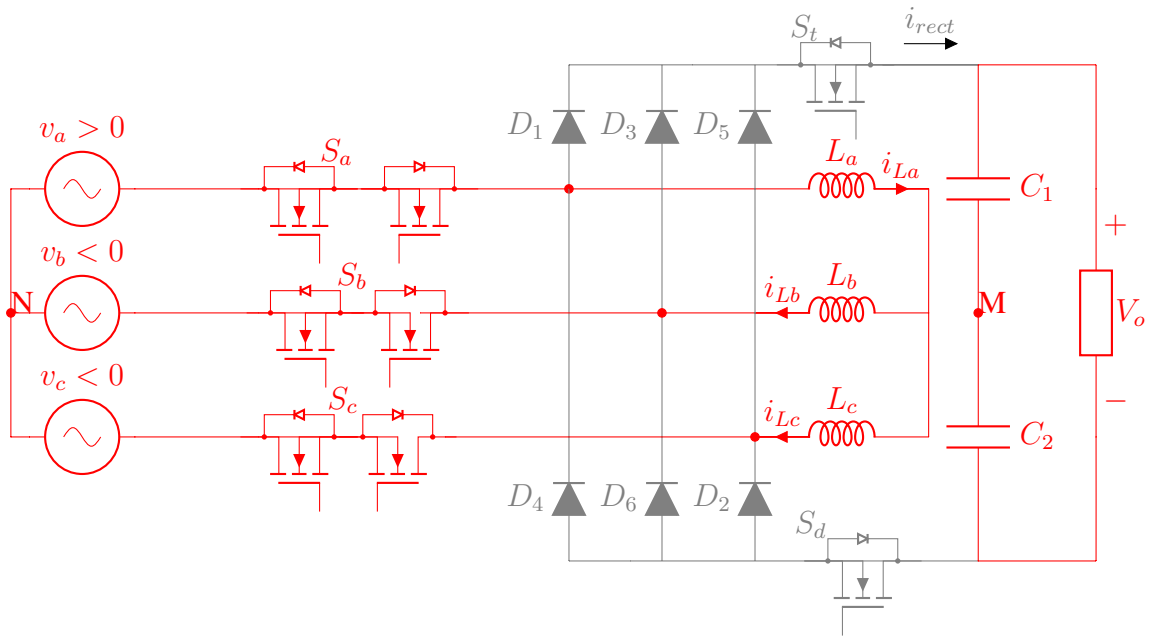

Figure 6.4: Equivalent circuit of Mode-1

6.3.2 Mode-2

In this mode of operation, gate pulses to the AC-side switches S_a, S_b, and S_c are removed and DC-side top and bottom switches S_t, S_d are ON. The energy stored in the three buck-boost inductors L_a, L_b, and L_c is transferred through the diode bridge to the DC side. This mode ends when the current in the inductor that started this interval with the lowest absolute current value reaches zero. Voltage that appeared across the switch(V_{S_a}) is $V_{S_a} = v_a + V_o/2$

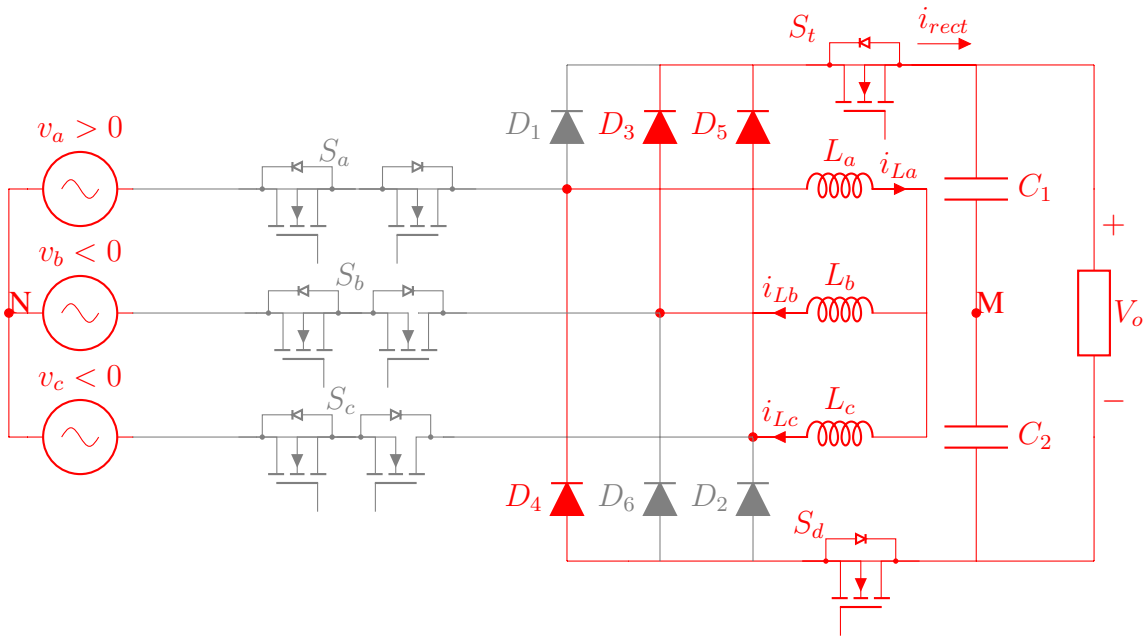

Figure 6.5: Equivalent circuit of Mode-2

6.3.3 Mode-3

In the second demagnetization mode, only the two inductors conduct current (L_a and L_c in the chosen example switching period) until their remaining magnetic energy has been transferred to the DC side, and hence their currents become zero, too.

6.3.4 Mode-4

Finally, the currents in all three inductors remain zero during mode-4, corresponding to DCM operation. The DC-side switches are turned off at the end of this mode directly before the next switching period starts.

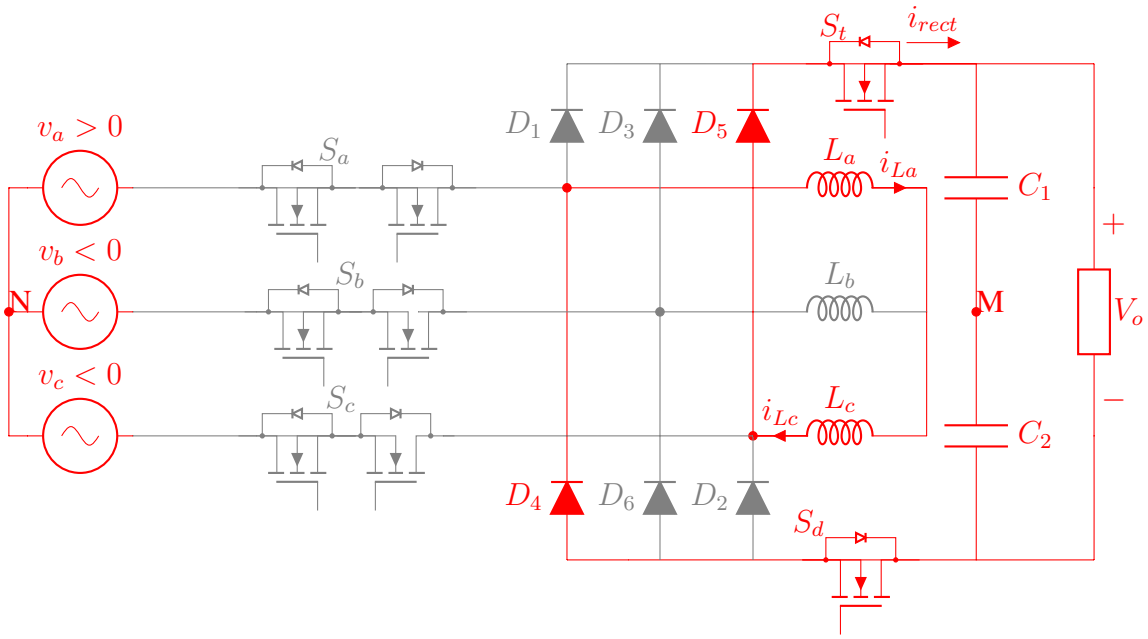

Figure 6.6: Equivalent circuit of Mode-3

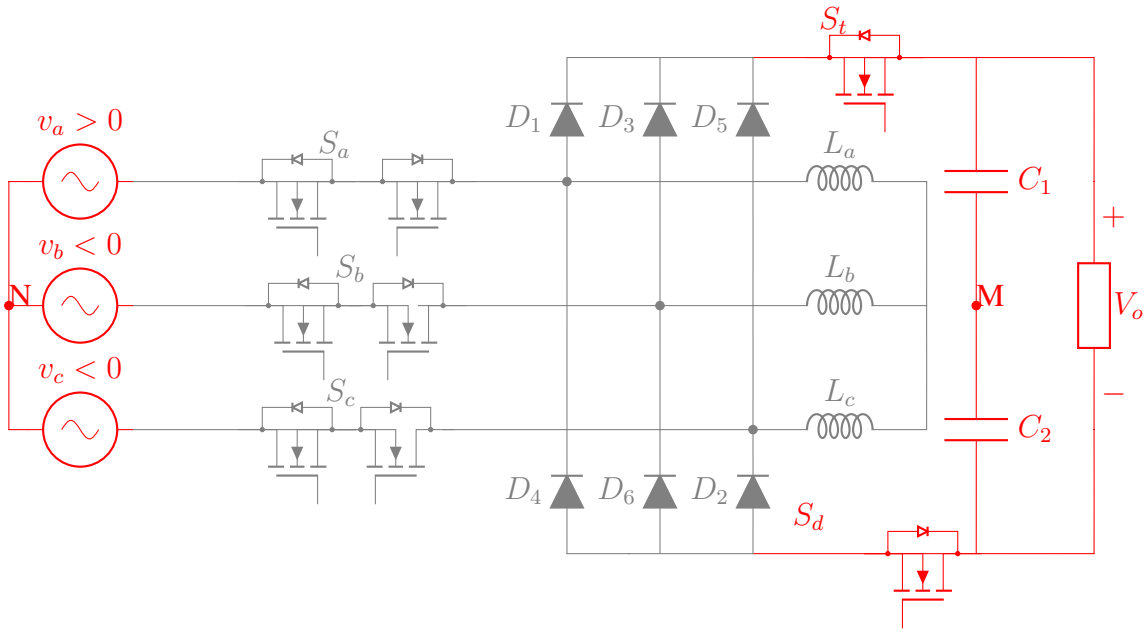

Figure 6.7: Equivalent circuit of Mode-4

Fig 6.8 shows the simulated waveforms at a particular line period where $v_a > 0$, $v_b < 0$ and $v_c < 0$.

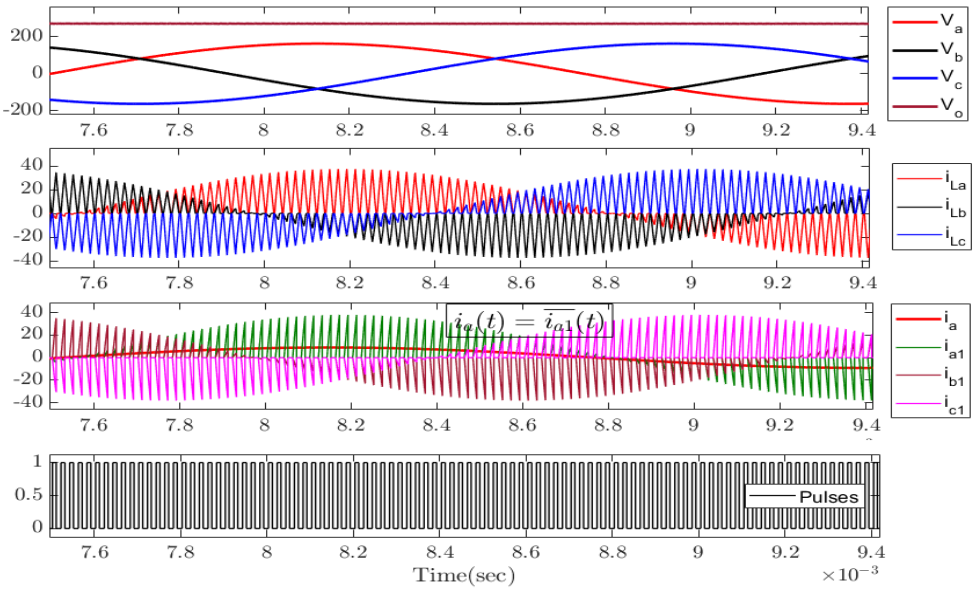

Figure 6.8: Simulated waveforms of the considered three phase buck–boost converter

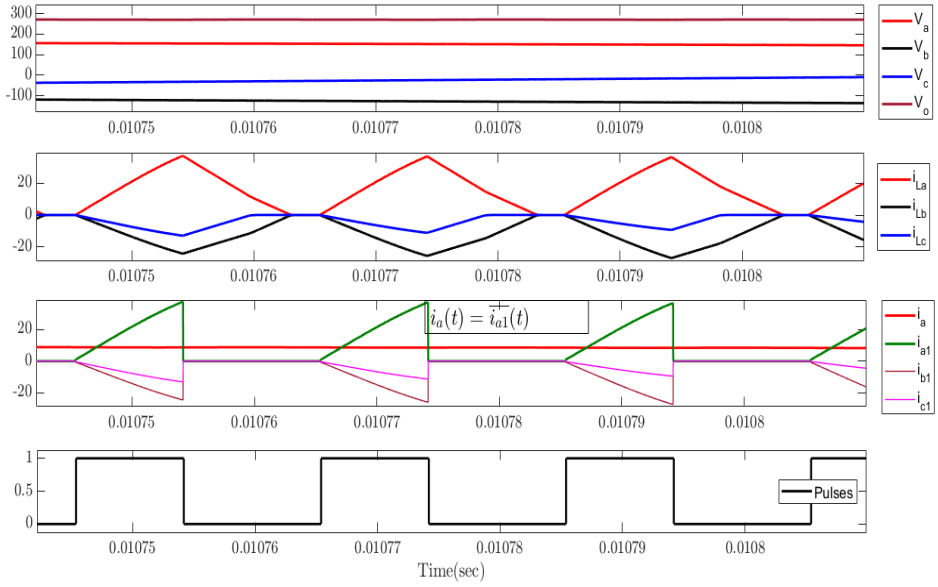

Figure 6.9: Magnified view of the simulated waveforms of the considered three phase buck–boost converter

6.4 Input Current

From Fig 6.9 considering phase-A (represented in green color), the local peak of the phase current $i_{a1}(t)$ varies over the mains period according to

$$\hat{i}_{a1}(t) = \frac{\overline{v_a}}{L_a} DT_s \tag{6.1}$$

All the inductors are assumed to be equal i.e $L_a = L_b = L_c = L$
The local average inductor current is given by

$$\overline{i_{a1}}(t) = \frac{D}{2}\hat{i}_{a1}(t) = \frac{D^2 T_s}{2L}\overline{v_a}(t) \tag{6.2}$$

Where $\overline{x}$ denotes the local average of x (i.e, the average over one switching cycle). Thus the local average of the phase current is proportional to phase volatge.

$$\overline{i_a}(t) = \frac{1}{R_{eq}}\overline{v_a}(t) \tag{6.3}$$

Therefore equation (6.3) shows the ohmic behaviour of the converter with three resistors connected in Y-configuration.

$$R_{eq} = \frac{2L}{D^2 T_s} \tag{6.4}$$

6.5 Power Transfer From AC-DC

Power transfer from AC-DC side is given by

$$P = 3\frac{\hat{v}_a^2}{R_{eq}} = \frac{V_{LL}^2}{R_{eq}} = \frac{V_{LL}^2 T_s}{2L} D^2 \tag{6.5}$$

Where $\hat{v}_a$ denotes the amplitude of phase voltage and V_{LL} is line-line RMS voltage,

$$\hat{v}_a = V_{LL}\sqrt{\frac{2}{3}}$$

Alternatively, the converter power transfer behaviour can be derived via the magnetic energy stored in the three inductors L. Assuming duty ratio (D) constant, the total en-

ergy stored in all the three inductors at end of Mode-1 is given by

$$E_{mag}(t) = \frac{L}{2}\left(\hat{i}_{a1}^2(t) + \hat{i}_{b1}^2(t) + \hat{i}_{c1}^2(t)\right)$$

$$E_{mag}(t) = \frac{L}{2}\left(\frac{\hat{V}_a D T_s}{L}\right)^2 \left(sin^2(\omega t) + sin^2(\omega t + \frac{2\pi}{3}) + sin^2(\omega t + \frac{4\pi}{3})\right) \quad (6.6)$$

$$E_{mag}(t) = \frac{\hat{V}_a^2 D^2 T_s^2}{2L}\frac{3}{2} = constant$$

Therefore from the above equation E_{mag} does not change over the mains period. Power transfer from AC-DC side is given by

$$P = \frac{E_{mag}(t)}{T_s} = \frac{V_{LL}^2 T_s}{2L} D^2 \quad (6.7)$$

Hence same equation (6.5) is obtained. The power transfer and output voltage, can therefore directly be controlled by adjusting a single parameter: the common duty ratio (D). Thus, the control circuitry can advantageously be of very simple structure and there is especially no need for any current sensors.

6.6 Ensuring DCM Operation

For ensuring DCM operation, all three inductors must be demagnetised completely within the time interval (1 - D) T_s i.e. energy stored E_{mag} i inductors must be completely transferred to the DC output during mode-2 and mode-3 intervals.

This demagnetization process is driven by the DC output voltage that is applied to an effective inductance L_{eq} formed by $L_a, L_b, and L_c$ and the diode rectifier. From Figs. 6.4 and 6.5, it can be seen that the equivalent inductance during the demagnetization depends on the current flow and is either L_{eq} = $\frac{3}{2}L$ (during mode-2 interval) or L_{eq} = 2L (during mode-3 interval). Hence, for the converter to operate in DCM, the inequality must satisfy

$$E_{mag}(t) < E_{demag}(t) \tag{6.8}$$

$$\frac{V_{LL}^2 T_s}{2L} D^2 < \frac{V_0^2 T_s}{L_{eq}^2} (1 - D)^2 \tag{6.9}$$

Clearly, the limiting case occurs for L_{eq} = 2 L, i.e. the case where one of the three-phase voltages equals zero, as the corresponding inductor current in the whole switching interval. Then, solving equation (6.9) for D gives

$$D < \frac{V_0}{V_o + \sqrt{2} V_{LL}} \tag{6.10}$$

This is the sufficient condition to ensure converter operate in DCM

6.7 Input Inductor Design

Inductor design is already discussed in chapter 3 in the same it is done here. The input inductor design is to be such that it has to maintain the DCM for minimum input voltage($V_{LL,min}$) and maximum output power(P_{max}) condition. Because at this condition, the converter input current is maximum, and consequently the inductor current peak also will be maximum. If the inductor can demagnetize within a switching period at this condition, then the DCM would be ensured for all the input voltages above the minimum input voltage and for all the output powers below rated power. Solving equation (6.7) for L and inserting (6.10) yield the upper limit for L that ensures DCM operation for the specified conditions.

From the equation (6.7)

$$L = \frac{V_{LL}^2 T_s}{2 P_{max}} D^2$$

Substituting the equation (6.10) in (6.7)

$$L < \frac{V_{LL}^2 T_s}{2 P_{max}} \left(\frac{V_o}{V_o + \sqrt{2} V_{LL,min}} \right)^2 \tag{6.11}$$

6.8 Maximum Power Transfer From AC-DC

For a given system, the above equation (6.11) can be rearranged to calculate the maximum power that can be transferred while maintaining DCM operation is given by

$$P_{max} = \frac{V_{LL,min}^2 T_s}{2L} \left(\frac{V_o}{V_o + \sqrt{2} V_{LL,min}} \right)^2 \tag{6.12}$$

6.9 Calculation of Design Parameters

Design parameters input inductor(L), duty ratio(D) define the converter to operate in DCM . These parameters are calculated from the following specifications.

Table 6.1: Input Specifications of PFC Converter

Parameter	**Value**
Line-Line voltage, V_{LLrms}	200V $\pm$ 15%
Input frequency, f	400Hz
Output power, P_o	2kW
Output voltage, V_o	270V
Switching frequency, f_s	50kHz

6.9.1 Duty Ratio (D)

From the equation (6.10)

$$D_{max} \leq \frac{V_o}{V_o + \sqrt{2} VLL, min}$$

$$V_o = 270$$

$$V_{LL} = 200 \pm 15\%$$

$$V_{LL,min} = 170V \qquad V_{LL,max} = 230V$$

$$D_{max} \leq \frac{270}{270 + \sqrt{2}(170)}$$

$$D_{max} \leq 0.528$$

D = 0.45 is considered for the simulation

6.9.2 Input Inductance

From the equation (6.11)

$$L < \frac{V_{LL}^2 T_s}{2P_{max}} \left(\frac{V_o}{V_o + \sqrt{2} V_{LL,min}} \right)^2$$

Substituting all the variables in the above equation we have the maximum inductance value required to operate the converter always in DCM i.e

$$L \leq 58uH$$

L = $40uH$ chosen for simulation.

Table 6.2: Design Parameters

Parameter	**Value**
Maximum Duty cycle, D_{max}	0.528
Input inductor, L	40μH
Load resistance, R	36.45
Output capacitor, C	200 μF
Duty cycle	0.45

In this chapter, three-phase buck-boost PFC converter with inductors connected in star-configuration is analysed. Basic operating modes, power transfer capability, calculation of design parameters for ensuring DCM operation of the converter are discussed in detail.

CHAPTER 7

Simulation Study of Three Phase Buck-Boost PFC Converter With Inductors in Y-Connection

2 kW, 400 Hz, 200 V AC RMS/ 270 V DC Three phase buck-boost PFC converter which is extension to the state-of-the-art topology is simulated in MATLAB/SIMULINK. Relevant waveforms which shows the characteristics of the converter are presented.

7.1 Input Voltage and Input Current

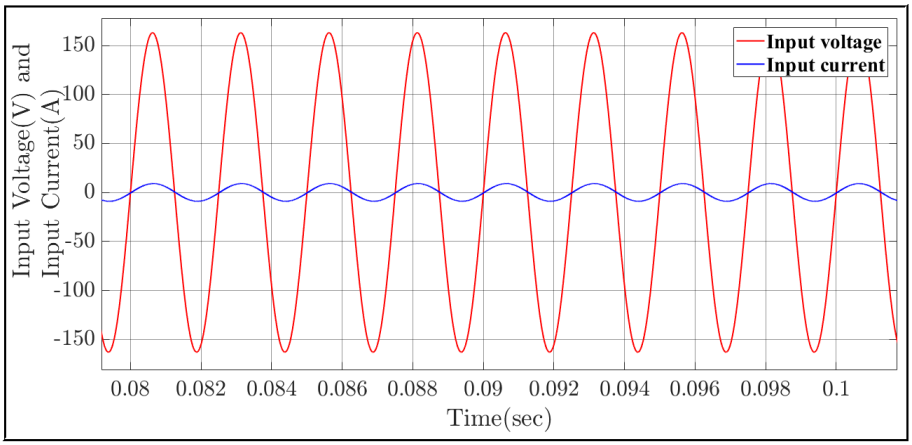

Figure 7.1: Input phase voltage and Input phase current of Phase-A

From the above Fig 7.1, it can be observed that input current $i_a(t)$ is sinusoidal and is in phase with the input voltage $v_a(t)$ of phase-a.

7.2 Three Phase Inductor Currents

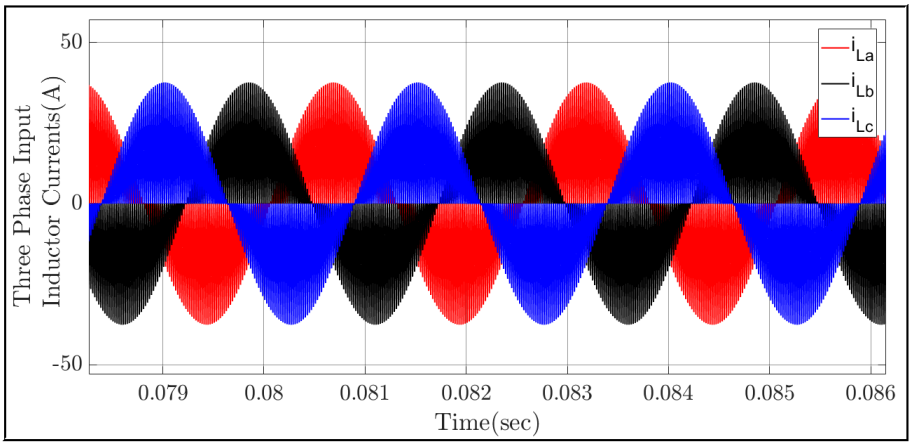

Figure 7.2: Three phase Inductor Currents

When all the three AC side switches are ON, three inductors L_a, L_b, L_c come across the phase voltages v_a, v_b, v_c respectively. Consequently, the inductor currents i_{La}, i_{Lb}, i_{Lc} begin simultaneously to rise from zero at a rate proportional to the instantaneous values of their respective phase voltages. The specific inductor peak current values during each ON interval are proportional to the average values of their input phase voltages during the same ON interval. Since each of these phase voltage average values vary sinusoidally, the inductor current peak and average values also vary sinusoidally as shown in Fig 7.2. Subsequently, the phase currents i_a, i_b, i_c average values also vary sinusoidally.

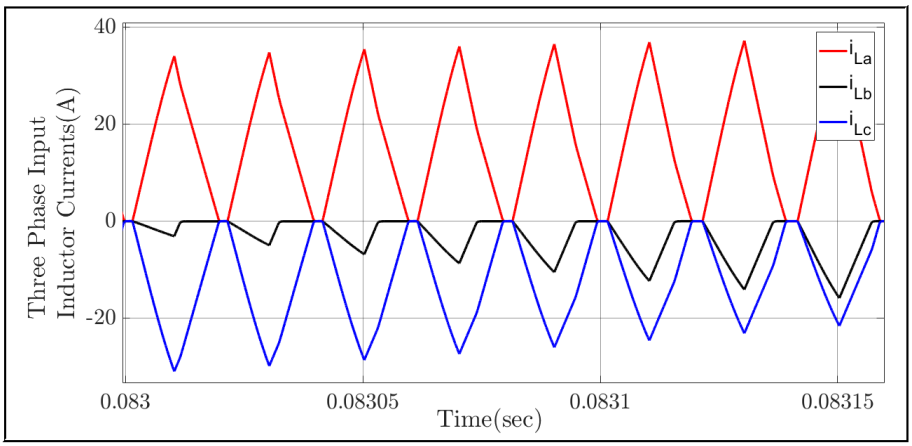

Figure 7.3: Magnified view of inductor currents

Fig 7.3 shows the magnified view of inductor currents operating in four modes of intervals i.e magnetising interval, two demagnetising intervals and the last discontinuous

conduction interval.

7.3 Voltage Stress in Switches

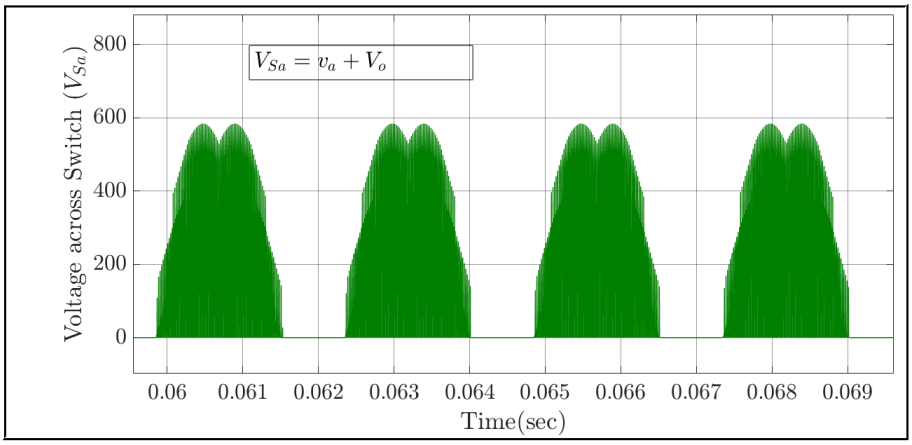

Figure 7.4: Voltage stress of AC-side switch in state-of-the-art topology

In the state of the art topology the peak blocking voltage applied to the AC-side switches (during the diode bridge conduction modes 2 and 3) amounts to the peak value of the line-to-line voltage plus the output voltage i.e $V_{Sa} = \sqrt{2}V_{LL} + V_o$ and maximum Voltage stress across DC side switches is $V_{St,Sd} = \sqrt{2}V_{LL} - V_0$

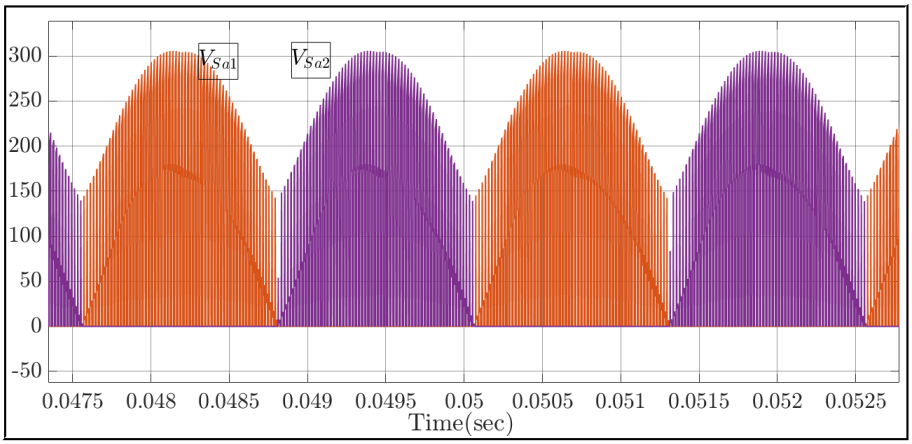

Figure 7.5: Voltage stress of AC-side switch in the extension to the state-of-the-art topology

In the extension to the state of the art topology back-to-back series connected switches are implemented and mid point (M)of the DC output side is connected to capacitor neutral N_f formed by AC-side filter capacitors. This connection can either be direct or, alternatively, a series resistor–capacitor (RC) element can be inserted in order to damp

transient oscillations if required. This connection ties the reference potential of the DC output to the star point and reduces the voltage stress of the DC-side switches from $V_{St,Sd} = \sqrt{2}V_{LL} - V_0$ to $V_{St,Sd} = \sqrt{2/3}V_{LL} - V_0/2$ and also the maximum blocking voltage stress of the AC-side switches is (ideally) reduced to $V_{Sa} = \sqrt{2/3}V_{LL} + V_0/2$.

7.4 Common Mode Voltage

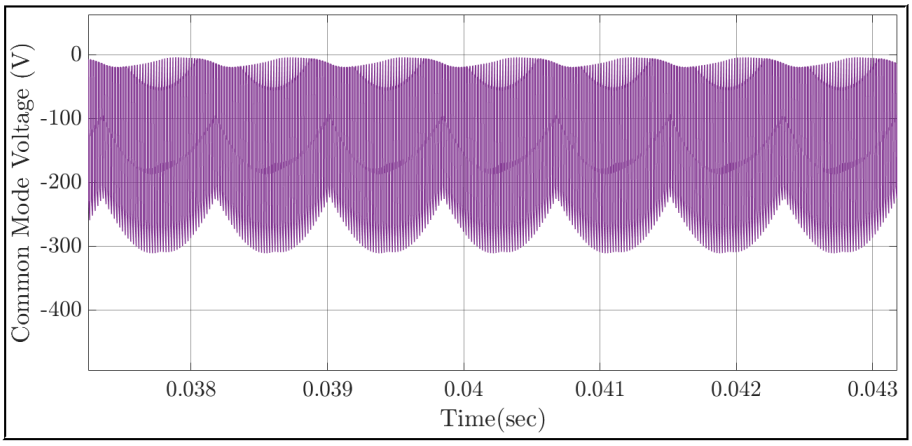

Figure 7.6: Common Mode voltage (V_{MN})in state-of-the-art topology

In the state-of-the-art topology, there is a switching-frequency Common Mode voltage between the midpoint of the DC output voltage (M) and the (grounded) star point neutral (N). During the magnetisation interval the most negative phase voltage is connected to the negative DC terminal via the corresponding diode (any current flow is prevented by S_t). However, because of the current directions in the buck–boost inductors L_a, L_b and L_c the upper diode of the bridge leg becomes conducting during the first demagnetisation interval. This connects the most negative phase voltage to the positive DC terminal since the AC-side switch of this phase cannot block any voltage in the required direction due to the anti-parallel diode. Therefore, the CM voltage undergoes a fast transition with a magnitude of V_o. From Fig 7.6 it can be observed that common mode voltage V_{MN} is present in state of the art topology.

In the extension to the basic topology, the midpoint (M) of the output voltage is connected to a capacitive star point N_f, which is formed by the AC-side filter capacitors. This connection can either be direct or, alternatively, a series resistor–capacitor (RC) element can be inserted in order to damp transient oscillations if required. This

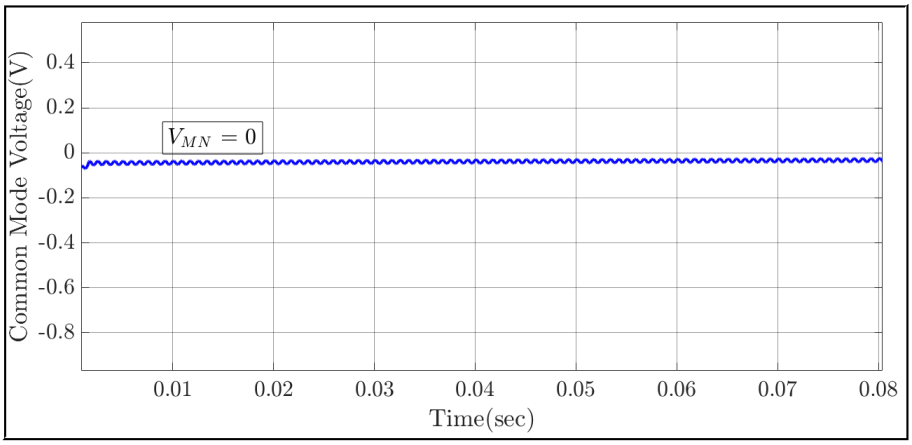

Figure 7.7: Common Mode voltage (V_{MN})in extension to the state-of-the-art topology

connection reduces the Common Mode voltage i.e V_{MN} = 0 as shown in the Fig 7.7.

7.5 Output Voltage

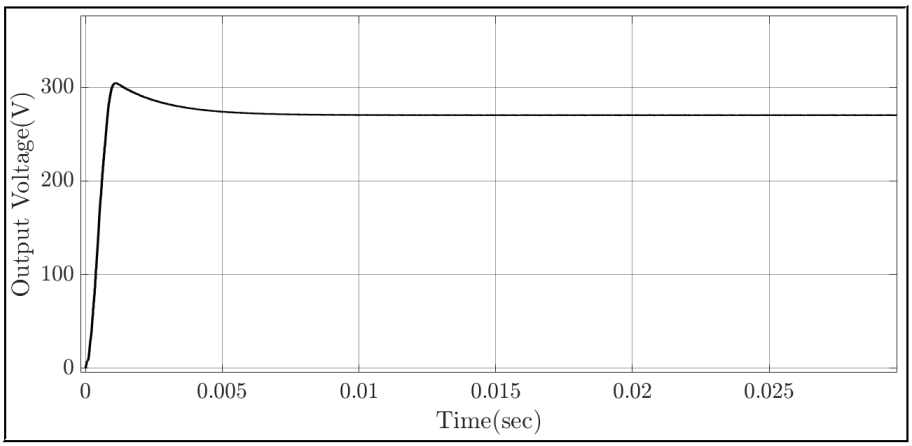

Figure 7.8: Output Voltage

Output voltage is reaching the desired value of 270V

7.6 Input Current THD

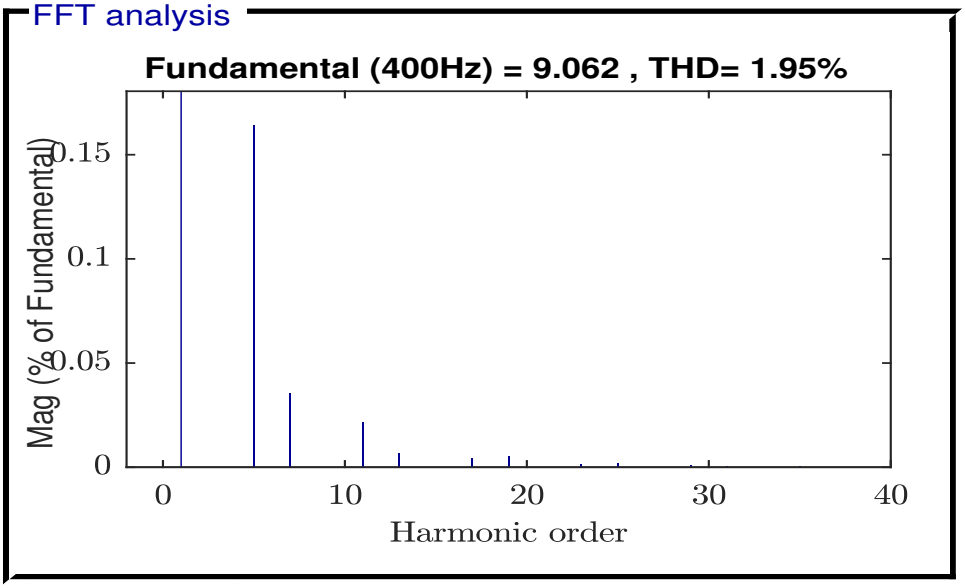

Figure 7.9: Input Current THD of extended state of the art topology

From the Fig 7.9 it is verified that all the input current harmonics are with in the aircraft standard DO160F limits and THD is 1.95% which is well below the standard THD limit.

In this chapter, problems associated with the state-of-the-art topology such as voltage stress across the switches, high frequency common mode voltage, and isolation between input AC-side and output DC-side are mitigated in the extension topology, same is shown in the simulation results.

CHAPTER 8

Conclusion

Based on a case study of unidirectional three-phase converter topologies, two converters, three-phase buck-boost derived PFC converter with input inductors connected in Δ and Y- configurations are selected and analyzed with regard to More electric aircraft applications. Both the topologies have advantages by operating the converters in DCM, Duty ratio(D) is the only parameter to control hence control is very simple. By operating in DCM, it eliminates the inner current control loop. Simple voltage control is sufficient. Due to the DCM operation, the converters require high rated current switches. However, the advantages of the converter such as less number of components, less number of sensors, and less control complexity significantly outweigh the disadvantage of high rated switches. The main features of individual topologies are discussed below.

Three phase Buck-Boost PFC Converter with Δ-configuration

- Input inductors connected in Δ as it results in 20% less peak inductor current when compared to Y-connection.
- Incase of phase loss or open switch fault all three inductors participate in power transfer.
- During phase loss this converter is able to deliver half the rated power.
- Small size low pass filter is sufficient to eliminate high order harmonics.
- Voltage stress across AC-side switches is more i.e $\sqrt{3}V_m + V_0$. so, high voltage rated switches are needed.
- Due to absence of DC side bi-directional switches, AC mains is directly connected to output DC.
- Common mode voltage issue is not Addressed in this topology.
- DC- side bi-directional switches are not required for the voltages levels when $\sqrt{2}V_{LL} > V_O$. As this condition avoids the conduction of diodes.
- This topology is best suitable for voltage levels when peak AC input voltage is less than the DC output voltage.

Three phase Buck-Boost PFC Converter with Y-configuration

- Incase of single-phase failure or open switch fault only two inductors will participate in power transfer and not able to deliver half the rated power.
- Back-to-back connected anti series bi-directional switches are implemented to reduce the voltage stress across AC-side switches.
- Bi-directional switches are connected both top and bottom at the DC-side. which isolates the AC mains and the output DC.
- Mid-point of the output is connected to Input capacitor Y-connected AC filter, which reduces the voltage stress across DC-side switches.
- Mid-point of the output DC-side is connected to capacitor neutral formed by AC-side filter capacitors. This connection can either be direct or alternatively, a series resistor-capacitor (RC) element can be inserted. This connection reduces the Common mode transient oscillations.
- This PFC rectifier topology is best suitable for applications of grid-connected converters, aircraft applications. This topology can operate with a wide frequency range of 50 Hz- 1000 Hz.

8.1 Future Scope

With an increasing demand for the more electric aircraft and All-electric aircraft, more efficient, reliable, high-performance power electronic converters are required.

This thesis work is mainly focused on the analysis of three-phase buck-boost PFC converter topologies suitable for aircraft systems are presented. The topologies are validated through simulations and the performance is better than the conventional power converters. In future research work, the new semiconductor devices such as SiC/GaN can be implemented and performance improvement needs to be evaluated. In this work all the switching devices, components are considered ideal in the analysis, further work can be carried by taking all the parasitics into consideration. Operating in high switching frequency reduces size and volume of components but it also increases switching losses resulting in large heat-sinks in hardware implementation. In DCM operation switches experience high current stress so Predictive control technique can be implemented as the Only parameter to control is duty ratio(D).

REFERENCES

[1] Michael Hartmann. *Ultra-compact and ultra-efficient three-phase PWM rectifier systems for more electric aircraft*. PhD thesis, ETH Zurich, 2011.

[2] Amit Kumar Singh. *Analysis and Design of Power Converter Topologies for Application in Future More Electric Aircraft*. Springer, 2018.

[3] Mohamad Hussien Taha. Power electronics application for more electric aircraft. *Recent Advances in Aircraft Technology*, 14:289–308, 2012.

[4] Johann Minibock and Johann W Kolar. Novel concept for mains voltage proportional input current shaping of a vienna rectifier eliminating controller multipliers. *IEEE Transactions on Industrial Electronics*, 52(1):162–170, 2005.

[5] Miniboeck Hartmann, J Miniboeck, and Johann W Kolar. A three-phase delta switch rectifier for more electric aircraft applications employing a novel pwm current control concept. In *2009 Twenty-Fourth Annual IEEE Applied Power Electronics Conference and Exposition*, pages 1633–1640. IEEE, 2009.

[6] Sivanagaraju Gangavarapu and Akshay K Rathore. Three-phase buck–boost derived pfc converter for more electric aircraft. *IEEE Transactions on Power Electronics*, 34(7):6264–6275, 2018.

[7] PRK Chetty. Current injected equivalent circuit approach to modeling of switching dc-dc converters in discontinuous inductor conduction mode. *IEEE Transactions on industrial electronics*, (3):230–234, 1982.

[8] Robert W Erickson and Dragan Maksimovic. *Fundamentals of power electronics*. Springer Science & Business Media, 2007.

[9] C-T Pan and T-C Chen. Step-up/down three-phase ac to dc convertor with sinusoidal input current and unity power factor. *IEE Proceedings-Electric Power Applications*, 141(2):77–84, 1994.

[10] Johann Miniböck, Mario Mauerer, Jonas E Huber, and Johann W Kolar. Three-phase buck–boost pfc rectifier with common-mode free output voltage and low semiconductor blocking voltage stress. *IET Power Electronics*, 12(8):2022–2030, 2019.